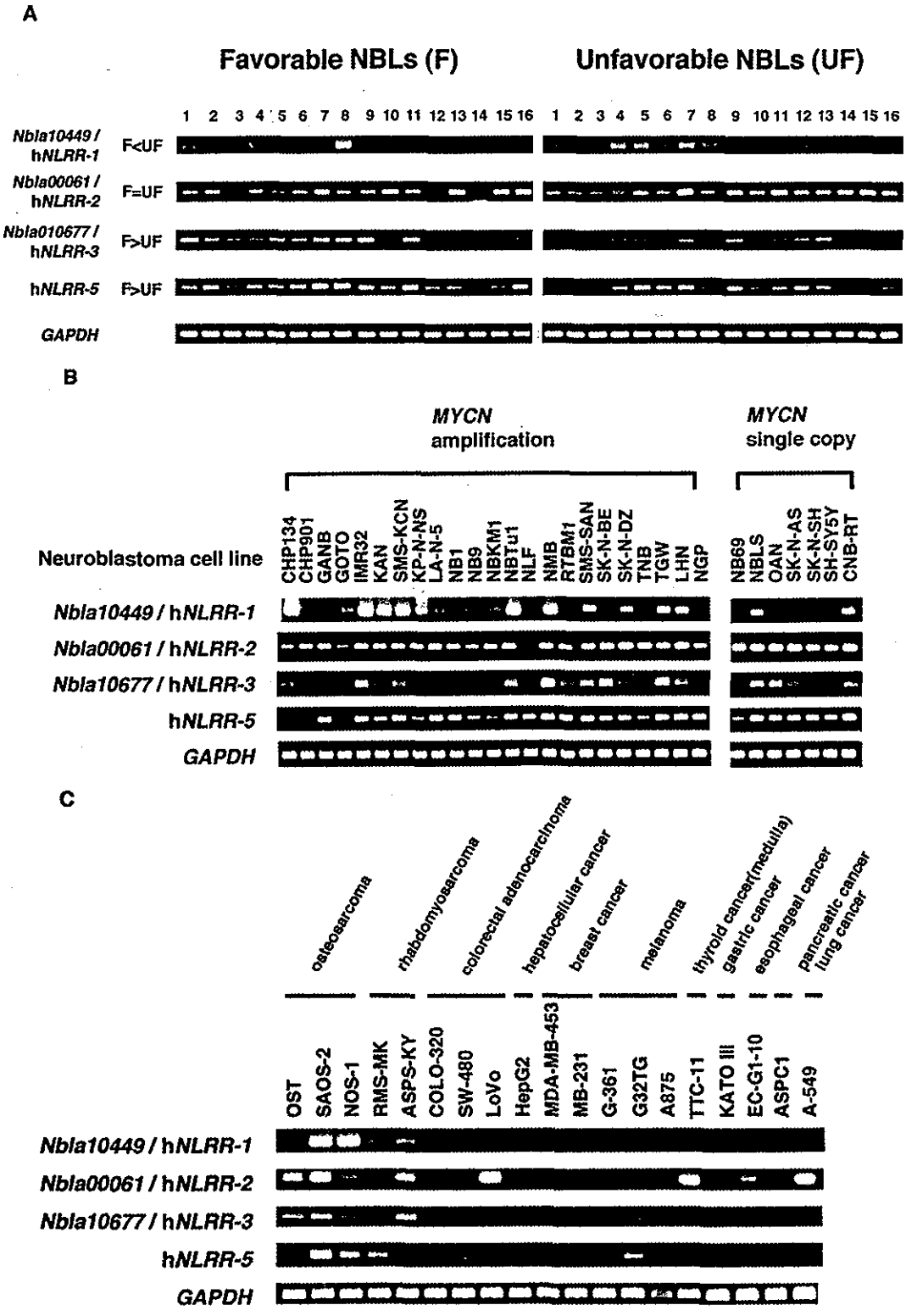

Figure 3. Expression of h*NLRR* family genes in primary NBLs, NBL cell lines and other cancer cell lines. A, Differential expression of h*NLRR* family genes in 16 favorable and 16 unfavorable NBLs. mRNA expression was detected by semi-quantitative RT-PCR procedure. The expression of *GAPDH* is shown as a control. Lanes 1-16: favorable NBLs (F, stage 1 or 2, with a single copy of *MYCN*), lanes 17-32: unfavorable NBLs (UF, stage 3 or 4, with *MYCN amplification*). B, Expression of h*NLRRs* mRNA in NBL cell lines. Twenty-three NBL cell lines with *MYCN* amplification and 7 cell lines with a single copy of *MYCN* were used for semi-quantitative RT-PCR as templates. C, Expression of h*NLRRs* mRNA in the other cancer cell lines. *Semi-quantitative* RT-PCR analysis was performed using cDNA and control *GAPDH* primers. Tumor origins are shown on the top.

expression by age, tumor stage, *TrkA* expression, *MYCN* copy number, origin, and mass screening. High expression of h*NLRR-1/Nbla10449* were significantly associated with >1 year of age (p=0.0001), advanced stage (p=0.0007), low expression of *TrkA* (p=0.011), *MYCN* amplification (p=0.0001) and sporadic tumors (p=0.0004), but not with the tumor origin (p=0.4). The results of log-rank test showed that a high level of h*NLRR-1/Nbla10449* expression was significantly associated

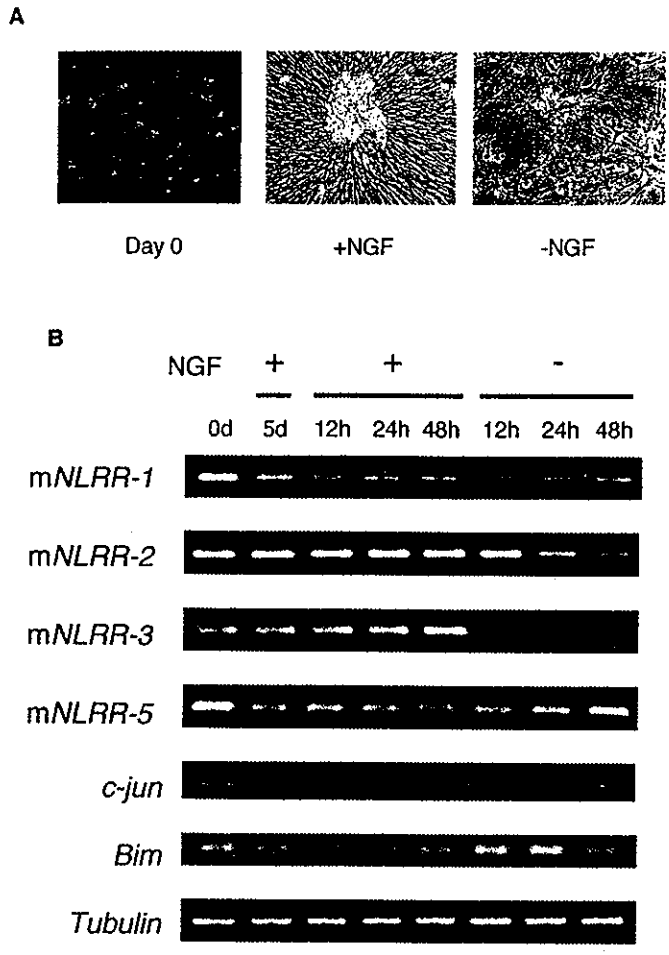

Figure 4. Changes in mRNA expression of mouse *NLRR* family genes in mouse superior cervical ganglion (SCG) cells treated with NGF in primary culture. A, Effect of NGF on newborn mouse SCG neurons in primary culture. The pictures were taken on day 0 and 5 (NGF^+) in the presence of 50 ng/ml NGF. NGF was then depleted from the medium by adding 1% v/v anti-NGF antibody for 36 h (NGF^-). B, Changes in expression of m*NLRR*s mRNA during NGF-induced differentiation and NGF depletion-induced apoptosis in newborn mouse SCG neurons in primary culture. SCG neurons were cultured for 5 days with NGF and then further cultured with or without NGF for 12, 24, 48 h. *c-jun* and *Bim*, positive control gene; Tubulin, used for standardization of the cDNA concentration.

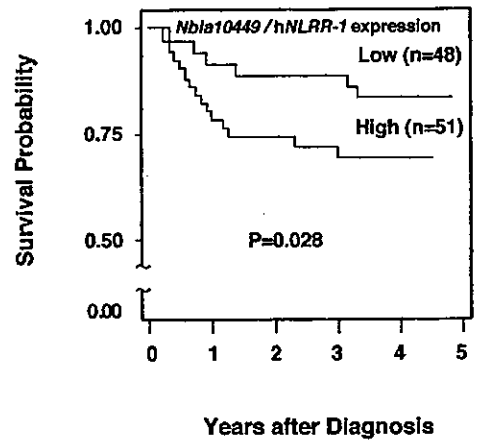

Figure 5. Kaplan-Meier survival curves for the 48 patients with low expression and the 51 patients with high expression.

with an unfavorable outcome (p=0.028). On the other hand, there was significant correlation between high levels of *Nbla10677/hNLRR-3* expression and younger age (p=0.0018), favorable stage (p=0.0007), high levels of *TrkA* expression (p=0.021), single copy of *MYCN* (p=0.0002) and the tumors found by mass screening (p=0.0049), but not with the tumor origin (p=0.33).

The univariate Cox regression was employed to examine the individual relationship of each variable to survival (Table II). These variables were: h*NLRR-1/Nbla10449* (log), h*NLRR-3/Nbla10677* (log), age (>1 year vs. <1 year), tumor stage (3+4 vs. 1+2+4s, *MYCN* copy number (1 copy vs. >1 copy), mass screening (+ vs. -), and origin (adrenal gland vs. others). Expression of h*NLRR-1/Nbla10449* (p=0.005), age (p<0.0005), *MYCN* copy number (p<0.0005), mass screening (p=0.001) were found to be statistically of prognostic importance. The results in Table II show that h*NLRR-1/Nbla10449* expression was an independent prognostic factor from age, *MYCN* copy number and mass screening in primary NBLs.

Discussion

In the present study, we identified the full-length human neuronal leucine-rich repeat protein (*NLRR*) family genes preferentially expressed in the nervous system and adrenal gland: *Nbla10449/hNLRR-1*, *Nbla00061/hNLRR-2/GAC1*, *Nbla10677/hNLRR-3* and h*NLRR-5*. In primary NBLs, the levels of h*NLRR-1* expression are significantly higher in the unfavorable subsets than those in the favorable tumors, whereas the expression pattern of h*NLRR-3* and h*NLRR-5* is the opposite. The results from the experiments using mouse SCG neurons treated with NGF in the primary culture have suggested that both m*NLRR-2* and *NLRR-3* are the molecules relating to promotion of neuronal survival or differentiation, while m*NLRR-1* and m*NLRR-5* function as those promoting cell growth or enhancing apoptosis. Furthermore, expression of h*NLRR-1* has been found as a significant indicator of poor outcome of NBLs, whereas that of h*NLRR-3* is associated with other favorable prognostic factors. Thus, hNLRR family members appear to differently regulate functions of neuronal cells as well as those of neuroblastoma.

A protein with leucine-rich repeat (LRR) domains was first identified in an α-2-glycoprotein of human serum (17). LRR-containing proteins represent a diverse group of molecules with different functions and cellular locations in a variety of organs. LRR domains provide an ideal conformation for binding to other proteins and this structure is thought to be involved in protein-protein interaction (10). Many LRR-containing proteins have been shown to function as cell-adhesion molecules or signaling receptors and are implicated in a variety of events in neural development. For example, adhesive LRR-containing proteins and small proteoglycans such as osteoinductive factor (OIF) bind various components of the extracellular matrix and growth factors. Interestingly, OIF binds the transforming growth factors, TGF-ß and TGF-ß2, and is involved in bone formation (18). The neurotrophin receptors, Trks, also possess the LRR domains in the extra-

Table I. Correlation between expression of *Nbla10449/hNLRR-1* or *Nbla10677/hNLRR-3* and other prognostic factors (Student's t-test).

Variable	No.	*Nbla10449/hNLRR-1* Mean ± SEM	*Nbla10449/hNLRR-1* p-value	*Nbla10677/hNLRR-3* Mean ± SEM	*Nbla10677/hNLRR-3* p-value
Age					
<1 year	63	0.84±0.21	0.0001	5.05±0.93	0.0018
>1 year	36	3.97±1.44		2.53±0.77	
Tumor stage					
1, 2, 4s	57	0.68±0.17	0.0007	5.36±1.00	0.0007
3, 4	42	3.74±1.25		2.48±0.68	
TrkA expression					
Low	45	3.50±1.17	0.011	3.13±0.77	0.021
High	54	0.71±0.18		4.97±1.02	
MYCN copy no.					
Amplified	29	5.19±1.75	0.0001	1.71±0.90	0.0002
Single	70	0.65±0.14		5.14±0.86	
Origin					
Adrenal gland	63	2.16±0.75	0.4	4.18±0.90	0.33
Others	36	1.67±0.79		4.06±0.93	
Mass screening					
+	54	0.67±0.18	0.0004	5.09±1.02	0.0049
-	45	3.55±1.17		2.98±0.76	

Table II. Cox regression models using *Nbla10449/hNLRR-1* expression and dichotomous factors of age, *TrkA* expression, *MYCN* amplification, and origin (n=99).

Model	Variable	p-value
A	*Nbla10449/hNLRR-1*	0.005
B	*Nbla10677/hNLRR-3*	0.15
C	Age (>1 vs. <1 year)	<0.005
D	*MYCN* (1 copy vs. amplification)	<0.005
E	Origin (adrenal gland vs. others)	0.079
F	Mass screening (+ vs. -)	0.001

cellular region. In *Drosophila*, some LRR domain-containing molecules such as toll, slit, connectin, chaoptin and tartan play an important role in regulating neural development (19-23).

The LRR motif includes highly hydrophobic amino acids and a repeat structure consisting of about 24 residues (20). NLRR family proteins contain in its extracellular region an immunoglobulin C-2 type domain and a fibronectin type III domain in addition to 11 sets of LRR motif (24). *NLRR* family genes were first isolated from a mouse brain cDNA library (16,25), and then 3 distinct isoforms (m*NLRR-1*, m*NLRR-2* and m*NLRR-3*) have been identified in zebrafish, *Xenopus*, mouse, rat and *Macaca facicularis* (16,24-26). The function of these NLRR proteins is poorly understood except that expression of m*NLRR-3* was increased after cortical brain injury (27) and that *rNLRR-3* expression is regulated through the Ras-MAPK signaling pathway in fibroblasts (28).

The deduced amino acid sequences of hNLRRs are highly conserved in the domains of LRR, LRRNT, LRRCT, Igc2 and FNIII, except that h*NLRR-5* does not have the FNIII domain. Many LRR proteins with LRRNT and LRRCT domains have been proposed to function in the regulation of neural differentiation and/or developmental processes as adhesive proteins and/or receptors (10). In addition to LRR, the Igc2 and FNIII domains in the extracellular region are often found in the molecules expressed in the central nervous system (26) and in several neuronal cell-adhesion molecules of the immunoglobulin superfamily such as N-CAM and L1 (29). Although hNLRRs and other NLRRs have no known signaling domain in the cytoplasmic region, a number of conserved stretches are found (Fig. 1). Especially, NLRR-1 and NLRR-3 have been shown to have a conserved stretch of 11 amino acids (ELYPPLINLWE) with 2 clathrin mediated endocytosis motifs, a tyrosine-based signal conforming to the YXRF motif (30,31), and a dileucine-type motif (32). Endocytosis and recycling mechanisms are relevant for cell adhesion molecules like integrins during cell migration (33,34).

Although the function of NLRR protein is poorly understood, there are some clues in recent reports. mNLRR-3 expression is increased in layers 2-3 in cerebral cortex after cortical injury, suggesting that this molecule plays a role in

the regulation of synaptic re-organization (27). zNLRR has also been proposed to have function as a neuronal-specific adhesion molecule or soluble ligand binding receptor during regeneration of the zebrafish central nervous system after injury, because retinal ganglion cells and descending spinal cord neurons strongly increased expression of *zNLRR* after axotomy in the adult (24).

The SCG/NGF system utilized in this study also provides a helpful hint to consider the neuronal function of hNLRRs. NLRR-1 may be involved in growth promotion in NBL by suppressing neuronal differentiation according to the result showing that the expression of m*NLRR-1* is down-regulated when the cells were treated with NGF. On the other hand, NLRR-3 may play a role in regulating differentiation to extend neurites and in neuronal survival of NBL cells since the expression of m*NLRR-3* was up-regulated by NGF and down-regulated after deprivation of NGF. These results are consistent with their differential expression pattern between favorable and unfavorable subsets of NBL.

In favorable NBLs as well as the cell lines with a single copy of *MYCN*, h*NLRR-1* expression was low as compared with the *MYCN*-amplified cells, suggesting that MYCN could influence the h*NLRR-1* expression. Interestingly, we have identified MYCN transcription factor-binding motifs (E-boxes) in the promoter region of the *NLRR-1* gene. Like h*NLRR-3*, h*NLRR-2* may also be involved in controlling neural cell survival as supposed from the result obtained in the NGF/SCG system. Ubiquitous h*NLRR-2* expression in NBLs suggests that h*NLRR-2* plays a role in maintaining cell survival. Of interest, h*NLRR-2* is often amplified in glioma as described below. h*NLRR-5* shows similar change in expression to h*NLRR-1* in the system of NGF-treated SCG neurons, albeit it is highly expressed in favorable NBLs. This suggests that hNLRR-5 may function as a proapoptotic molecule in NBL. Thus, each hNLRR member may have distinct biological function in NBL as well as neuronal cells. As the deduced intracellular region at the extreme C-terminus of hNLRR proteins has variable amino acid sequences, it may play a role in determining the differential function of hNLRR family receptors.

There are a few reports showing the relationship between LRR or NLRR and human cancer. *GAC1* (*hNLRR-2*), mapped to chromosome 1q32.1, is amplified and overexpressed in glioblastoma multiforme and anaplastic astrocytoma (15). Another report shows that expression of r*NLRR-3*, which was cloned by the subtractive screening using fibrosarcoma cells overexpressing c-Ha-ras, is regulated through the Ras-MAPK pathway, albeit the role in cancer cells is unknown (28). Trk family receptor tyrosine kinases have 3 LRRs in the extracellular domain, whose alteration can cause onco genic activation in some cancers (35). Interestingly, TrkA and TrkB also show an inverse expression pattern between favorable and unfavorable NBLs, that is very similar to the pattern of h*NLRR-1* and h*NLRR-3* expression. Since expression levels of TrkA and TrkB are powerful prognostic factors in NBLs, those of h*NLRR-1* and h*NLRR-3* may also be important in predicting the patient's outcome. Indeed, our present data suggest that expression of both hNLRR-1 and hNLRR-3 is inversely associated with the prognosis as well as other prognostic factors.

Acknowledgements

The authors thank Drs M. Fukumura, and H. Tsunobuchi for helpful discussions, Drs H. Kageyama and K. Miyazaki for experimental support, Dr S. Sakiyama for encouragement, and Ms. N. Sugimitsu and A. Morohashi for their excellent technical assistance. The authors also thank the following institutes for providing surgical samples: First Department of Surgery, Hokkaido University School of Medicine; Department of Pediatrics, National Sapporo Hospital; Department of Pediatric Surgery, Tohoku University School of Medicine; Department of Surgery, Gunma Children's Medical Center; Department of Pediatrics, Pediatric Surgery and General Surgery, Jichi Medical University; Department of Hematology and Oncology, Saitama Children's Medical Center; Department of Pediatrics, Juntendo University School of Medicine; Department of Surgery, Kiyose Metropolitan Children's Hospital; Department of Surgery and Pathology, Chiba Children's Hospital; Department of Pediatric Surgery, Chiba University School of Medicine; Department of Pediatric Surgery, Kimitsu Central Hospital; Department of Pediatric Surgery, Niigata University School of Medicine; Department of Pediatrics and Pediatric Surgery, Aichi Medical University; Department of Pediatrics, Kyoto Prefectural Medical University; Tumor Board, Hyogo Children's Hospital; Department of Pediatrics and Pediatric Surgery, Kagoshima University School of Medicine; Department of Pediatric Surgery, Showa University School of Medicine; Department of Pediatrics, Oita University School of Medicine; Department of Pediatric Surgery, Ohta General Hospital; Department of Pediatrics, Ichinomiya City Hospital; Department of Pediatric Surgery, Osaka City General Hospital; Department of Pediatrics, Nihon University School of Medicine Itabashi Hospital; Department of Pediatric Surgery, University of Tsukuba School of Medicine.

References

1. Bolande RP: The neurocristopathies. A unifying concept of disease arising in neural crest maldevelopement. Hum Pathol 5: 409-429, 1974.
2. Lo L, Morin X, Brunet JF and Anderson DJ: Specification of neurotransmitter identity by Phox2 proteins in neural crest stem cells. Neuron 22: 693-705, 1999.
3. Nakagawara A, Arima-Nakagawara M, Scavarda NJ, Azar CG, Cantor AB and Brodeur GM: Association between high levels of expression of the TRK gene and favorable outcome in human neuroblastoma. N Engl J Med 328: 847-854, 1993.
4. Nakagawara A, Azar CG, Scavarda NJ and Brodeur GM: Expression and function of TRK-B and BDNF in human neuroblastomas. Mol Cell Biol 14: 759-767, 1994.
5. Lasorella A, Noseda M, Beyna M, Yokota Y and Iavarone A: Id2 is a retinoblastoma protein target and mediates signaling by Myc oncoprotein. Nature 407: 592-598, 2000.
6. Ohira M, Shishikura T, Kawamoto T, Inuzuka H, Morohashi A, Takayasu H, Kageyama H, Takada N, Takahashi M, Sakiyama S, Suzuki Y, Sugano S, Kuma H, Nozawa I and Nakagawara A: Hunting the subset-specific genes of neuroblastoma: expression profiling and differential screening of the full-length-enriched oligo-capping cDNA libraries. Med Pediatr Oncol 35: 547-549, 2000.
7. Suzuki Y, Yoshitomo-Nakagawa K, Maruyama K, Suyama A and Sugano S: Construction and characterization of a full length-enriched and a 5'-end-enriched cDNA library. Gene 200: 149-156, 1997.

8. Ohira M, Morohashi A, Inuzuka H, Shishikura T, Kawamoto T, Kageyama T, Nakamura Y, Isogai E, Takayasu H, Sakiyama S, Suzuki Y, Sugano S, Goto T, Sato S and Nakagawara A: Expression profiling and characterization of 4200 genes cloned from primary neuroblastomas: identification of 305 genes differentially expressed between favorable and unfavorable subsets. Oncogene 22: 5525-5536, 2003.
9. Ohira M, Morohashi A, Nakamura Y, Isogai E, Furuya K, Hamano S, Machida T, Aoyama, Fukumura M, Miyazaki K, Suzuki Y, Sugano S, Hirato J and Nakagawara A: Neuroblastoma oligo-capping cDNA project: toward the understanding of the genesis and biology of neuroblastoma. Cancer Lett 197: 63-68, 2003.
10. Kobe B and Deisenhofer J: The leucine-rich repeat: a versatile binding motif. Trends Biochem Sci 19: 415-421, 1994.
11. Shimada H, Chatten J, Newton WA Jr, Sachs N, Hamoudi AB, Chiba T, Marsden HB and Misugi K: Histopathologic prognostic factors in neuroblastic tumors: definition of subtypes of ganglioneuroblastoma and an age-linked classification of neuroblastomas. J Natl Cancer Inst 73: 405-416, 1984.
12. Brodeur GM, Pritchard J, Berthold F, Carlsen NL, Castel V, Castelberry RP, De Bernardi B, Evans AE, Favrot M and Hedborg F: Revisions of the international criteria for neuroblastoma diagnosis, staging and response to treatment. J Clin Oncol 11: 1466-1477, 1993.
13. Kaneko M, Nishihira H, Mugishima H, Ohnuma N, Nakada K, Kawa K, Fukuzawa M, Suita S, Sera Y and Tsuchida Y: Stratification of treatment of stage 4 neuroblastoma patients based on N-myc amplification status. Study Group of Japan for Treatment of Advanced Neuroblastoma, Tokyo, Japan. Med Pediatr Oncol 31: 1-7, 1998.
14. Smith CJ, Johnson EM Jr, Osborne P, Freeman RS and Neveu I and Brachet P: NGF deprivation and neuronal degeneration trigger altered beta-amyloid precursor protein gene expression in the rat superior cervical ganglia *in vivo* and *in vitro*. Brain Res Mol Brain Res 17: 328-334, 1993.
15. Almeida A, Zhu XX, Vogt N, Tyagi R, Muleris M, Dutrillaux AM, Dutrillaux B, Ross D, Malfoy B and Hanash S: GAC1, a new member of the leucine-rich repeat superfamily on chromosome band 1q32.1, is amplified and overexpressed in malignant gliomas. Oncogene 16: 2997-3002, 1998.
16. Taguchi A, Wanaka A, Mori T, Matsumoto K, Imai Y, Tagaki T and Tohyama M: Molecular cloning of novel leucine-rich repeat proteins and their expression in the developing mouse nervous system. Brain Res Mol Brain Res 35: 31-40, 1996.
17. Takahashi N, Takahashi Y and Putnam FW: Periodicity of leucine and tandem repetition of a 24-amino acid segment in the primary structure of leucine-rich alpha 2-glycoprotein of human serum. Proc Natl Acad Sci USA 82: 1906-1910, 1985.
18. Kresse H, Hausser H and Schonherr E: Small proteoglycans. Experientia 49: 403-416, 1993.
19. Lemaitre B, Nicolas E, Michaut L, Reichhart JM and Hoffmann JA: The dorsoventral regulatory gene cassette spatzle/Toll/cactus controls the potent antifungal response in *Drosophila* adults. Cell 86: 973-983, 1996.
20. Rothberg JM, Jacobs JR, Goodman CS and Artavanis-Tsakonas S: Slit: an extracellular protein necessary for development of midline glia and commissural axon pathways contains both EGF and LRR domains. Genes Dev 4: 2169-2187, 1990.
21. Nose A, Mahajan VB and Goodman CS: Connectin: a homophilic cell adhesion molecule expressed on a subset of muscles and the motoneurons that innervate them in *Drosophila*. Cell 70: 553-567, 1992.
22. Krantz DE and Zipursky SL: *Drosophila chaoptin*, a member of the leucine-rich repeat family, is a photoreceptor cell-specific adhesion molecule. EMBO J 9: 1969-1977, 1990.
23. Chang Z, Price BD, Bockheim S, Boedigheimer MJ, Smith R and Laughon A: Molecular and genetic characterization of the *Drosophila tartan gene*. Dev Biol 160: 315-332, 1993.
24. Bormann P, Roth LW, Andel D, Ackermann M and Reinhard E: zfNLRR, a novel leucine-rich repeat protein is preferentially expressed during regeneration in zebrafish. Mol Cell Neurosci 13: 167-179, 1999.
25. Taniguchi H, Tohyama M and Takagi T: Cloning and expression of a novel gene for a protein with leucine-rich repeats in the developing mouse nervous system. Brain Res Mol Brain Res 36: 45-52, 1996.
26. Hayata T, Uochi T and Asashima M: Molecular cloning of XNLRR-1, a *Xenopus* homolog of mouse neuronal leucine-rich repeat protein expressed in the developing *Xenopus* nervous system. Gene 221: 159-166, 1998.
27. Ishii N, Wanaka A and Tohyama M: Increased expression of NLRR-3 mRNA after cortical brain injury in mouse. Brain Res Mol Brain Res 40: 148-152, 1996.
28. Fukamachi K, Matsuoka Y, Kitanaka C, Kuchino Y and Tsuda H: Rat neuronal leucine-rich repeat protein-3: cloning and regulation of the gene expression. Biochem Biophys Res Commun 287: 257-263, 2001.
29. Brummendorf T and Rathjen FG: Structure/function relationships of axon-associated adhesion receptors of the immunoglobulin superfamily. Curr Opin Neurobiol 6: 584-593, 1996.
30. Chen WJ, Goldstein JL and Brown MS: NPXY, a sequence often found in cytoplasmic tails, is required for coated pit-mediated internalization of the low density lipoprotein receptor. J Biol Chem 265: 3116-3123, 1990.
31. Collawn JF, Stangel M, Kuhn LA, Esekogwu V, Jing SQ, Trowbridge IS and Tainer JA: Transferrin receptor internalization sequence YXRF implicates a tight turn as the structural recognition motif for endocytosis. Cell 63: 1061-1072, 1990.
32. Kirchhausen T: Clathrin. Annu Rev Biochem 69: 699-727, 2000.
33. Lauffenburger DA and Horwitz AF: Cell migration: a physically integrated molecular process. Cell 84: 359-369, 1996.
34. Lawson MA and Maxfield FR: Ca(2+)- and calcineurin-dependent recycling of an integrin to the front of migrating neutrophils. Nature 377: 75-79, 1995.
35. Meakin SO and Shooter EM: The nerve growth factor family of receptors. Trends Neurosci 15: 323-231, 1992.

THE JOURNAL OF BIOLOGICAL CHEMISTRY
Vol. 279, No. 12, Issue of March 19, pp. 11327–11335, 2004
Printed in U.S.A.

NEDL1, a Novel Ubiquitin-protein Isopeptide Ligase for Dishevelled-1, Targets Mutant Superoxide Dismutase-1*

Received for publication, November 12, 2003, and in revised form, December 16, 2003
Published, JBC Papers in Press, December 18, 2003, DOI 10.1074/jbc.M312389200

Kou Miyazaki‡, Tomoyuki Fujita‡, Toshinori Ozaki‡, Chiaki Kato‡, Yuka Kurose‡, Maya Sakamoto‡, Shinsuke Kato§, Takeshi Goto¶, Yasuto Itoyama‖, Masashi Aoki‖, and Akira Nakagawara‡

From the ‡Division of Biochemistry, Chiba Cancer Center Research Institute, Chiba 260-8717, Japan, the §Division of Neuropathology, Institute of Neurological Sciences, Faculty of Medicine, Tottori University, Yonago 683-8504, Japan, ¶Hisamitsu Pharmaceutical Company Incorporated, Tokyo 100-622, Japan, and the ‖Department of Neurology, Tohoku University School of Medicine, Sendai 980-8574, Japan

Approximately 20% of familial amyotrophic lateral sclerosis (FALS) arises from germ-line mutations in the superoxide dismutase-1 (*SOD1*) gene. However, the molecular mechanisms underlying the process have been elusive. Here, we show that a neuronal homologous to E6AP carboxyl terminus (HECT)-type ubiquitin-protein isopeptide ligase (NEDL1) physically binds translocon-associated protein-δ and also binds and ubiquitinates mutant (but not wild-type) SOD1 proportionately to the disease severity caused by that particular mutant. Immunohistochemically, NEDL1 is present in the central region of the Lewy body-like hyaline inclusions in the spinal cord ventral horn motor neurons of both FALS patients and mutant *SOD1* transgenic mice. Two-hybrid screening for the physiological targets of NEDL1 has identified Dishevelled-1, one of the key transducers in the Wnt signaling pathway. Mutant SOD1 also interacted with Dishevelled-1 in the presence of NEDL1 and caused its dysfunction. Thus, our results suggest that an adverse interaction among misfolded SOD1, NEDL1, translocon-associated protein-δ, and Dishevelled-1 forms a ubiquitinated protein complex that is included in potentially cytotoxic protein aggregates and that mutually affects their functions, leading to motor neuron death in FALS.

Amyotrophic lateral sclerosis (ALS)[1] is a progressive, fatal, neurodegenerative disease that is characterized by selective loss of motor neurons in the spinal cord, brain stem, and motor cortex. The sporadic and familial forms of the disease have similar clinical and pathological features. About 10% of ALS cases are familial, and mutation of superoxide dismutase-1 (SOD1) is found in 20% of familial ALS (FALS) patients (1, 2). Mice that express mutant *SOD1* transgenes develop an age-dependent ALS phenotype independent of levels of dismutase activity, suggesting that FALS pathology is because of a toxic gain of function in SOD1 and that the abnormal protein structure of mutant SOD1 is critical in the pathogenesis of motor neuron death (3–6). Recently, proteasome expression and activity have been reported to decrease with age in the spinal cord (7, 8). Furthermore, mutant SOD1 turns over more rapidly than wild-type SOD1, and an inhibitor of proteasome action inhibits this turnover and thus selectively increases the steady-state level of mutant SOD1 (8). These results suggest the involvement of the ubiquitin-proteasome function in the cause of FALS. However, the biochemical nature of this gain-of-function mutation in SOD1 and the mechanism by which SOD1 mutations cause the degeneration of motor neurons have remained elusive.

We show here the identification of a novel HECT-type ubiquitin-protein isopeptide ligase (E3), NEDL1, which is expressed in neuronal tissues, including the spinal cord, and selectively binds to and ubiquitinates mutant (but not wild-type) SOD1. NEDL1 is physically associated with translocon-associated protein-δ (TRAP-δ), one of the endoplasmic reticulum (ER) translocon components that has previously been reported to bind mutant SOD1 (9, 10). Both NEDL1 and TRAP-δ form a complex with mutant SOD1, with the binding intensity among these proteins being roughly proportionate to the rapidity of progression of the associated FALS phenotype. Immunohistochemical study has shown that NEDL1 is positive in the Lewy body-like hyaline inclusions in the spinal cord motor neurons of both FALS patients and mutant *SOD1* transgenic mice. We have also found that NEDL1 targets Dishevelled-1 (Dvl1) for ubiquitination-mediated degradation and that mutant (but not wild-type) SOD1 affects the function of Dvl1. Our observations suggest that NEDL1 is a quality control E3 that recognizes mutant SOD1 to form a tight complex with the physiological targets of NEDL1 in motor neurons of FALS patients.

EXPERIMENTAL PROCEDURES

Cell Culture and Transfection—Human neuroblastoma-derived cells were grown in RPMI 1640 medium supplemented with 10% heat-inactivated fetal bovine serum, 100 units/ml penicillin, and 100 μg/ml streptomycin. COS-7 and Neuro2a cells were maintained in Dulbecco's modified Eagle's medium supplemented with 10% heat-inactivated fe-

* This work was supported in part by Hisamitsu Pharmaceutical Co. Inc. (to A. N.), by grants from the Ministry of Health, Labor, and Welfare of Japan (to A. N. and Y. I.), and by grants from the Ministry of Education, Culture, Sports, Science, and Technology of Japan (to A. N., Y. I., and M. A.). The costs of publication of this article were defrayed in part by the payment of page charges. This article must therefore be hereby marked "*advertisement*" in accordance with 18 U.S.C. Section 1734 solely to indicate this fact.

The nucleotide sequence(s) reported in this paper has been submitted to the GenBank™/EBI Data Bank with accession number(s) AB048365 (Nbla0078 and human NEDL1), AB002320 (KIAA0322), and AB083710 (mouse Nedl1).

** To whom correspondence should be addressed: Div. of Biochemistry, Chiba Cancer Center Research Inst., 666-2 Nitona, Chuoh-ku, Chiba 260-8717, Japan. Tel.: 81-43-264-5431; Fax: 81-43-265-4459; E-mail: akiranak@chiba-ccri.chuo.chiba.jp.

[1] The abbreviations used are: ALS, amyotrophic lateral sclerosis; FALS, familial amyotrophic lateral sclerosis; SOD1, superoxide dismutase-1; E3, ubiquitin-protein isopeptide ligase; NEDL1, NEDD4-like ubiquitin-protein ligase-1; TRAP-δ, translocon-associated protein-δ; ER, endoplasmic reticulum; Dvl1, Dishevelled-1; RT, reverse transcription; LBHI, Lewy body-like hyaline inclusion; JNK, c-Jun N-terminal kinase; HECT domain, homologous to E6AP carboxyl-terminus.

tal bovine serum, 100 units/ml penicillin, and 100 μg/ml streptomycin. All cells were maintained in a humidified 37 °C incubator with 5% CO_2. All transfections were carried out with LipofectAMINE Plus transfection reagent (Invitrogen) according to the manufacturer's instructions. In some experiments, transfected cells were treated with MG-132 for 30 min at a final concentration of 40 μM.

RNA Analysis—A human multiple tissue mRNA blot and a fetal human multiple mRNA blot (Invitrogen) were hybridized with a ^{32}P-labeled ApaI-ScaI restriction fragment of *NEDL1* cDNA under standard conditions. For reverse transcription (RT)-PCR analysis, cDNA derived from adult human neural system (BioChain Institute, Hayward, CA) was subjected to PCR amplification using the following primers: *NEDL1*, 5′-CCGATTTGAGATCACTTCCTCC-3′ (sense) and 5′-CCGCTTTCCATCAGGTTGTT-3′ (antisense); and glyceraldehyde-3-phosphate dehydrogenase, 5′-ACCTGACCTGCCGTCTAGAA-3′ (sense) and 5′-TCCACCACCCTGTTGCTGTA-3′ (antisense). The amplified products were separated by electrophoresis on a 1.5% agarose gel and visualized by ethidium bromide post-staining. Amplification of glyceraldehyde-3-phosphate dehydrogenase was used as an internal control.

In Vitro Ubiquitination Assays—*In vitro* ubiquitination assays were performed as follows. Reaction mixtures containing 0.5 μg of purified glutathione *S*-transferase fusion proteins, 0.25 μg of yeast ubiquitin-activating enzyme (*E1*) (BostonBiochem, Cambridge, MA), 1 μl of crude lysates from *Escherichia coli* expressing ubiquitin carrier proteins (*E2*), and 10 μg of bovine ubiquitin (Sigma) were incubated in 250 mM Tris-HCl (pH 7.6), 1.2 M NaCl, 50 mM ATP, 10 mM $MgCl_2$, and 30 mM dithiothreitol. Reactions were terminated after 2 h at 30 °C by the addition of SDS sample buffer. Samples were resolved by SDS-PAGE, transferred to membranes, and immunoblotted with anti-ubiquitin monoclonal antibody 1B3 (Medical & Biological Laboratories, Nagoya, Japan).

Immunofluorescence Staining—Cells grown on coverslips were processed for immunofluorescence. Briefly, cells were fixed in 3.7% formaldehyde, permeabilized in 0.2% Triton X-100, and finally incubated with anti-NEDL1 antibody (diluted 1:100). The primary antibody was detected with fluorescein isothiocyanate-conjugated goat anti-rabbit IgG (diluted 1:500; Jackson ImmunoResearch Laboratories, Inc., West Grove, PA). Images were taken using an Olympus confocal microscopy system.

Yeast Two-hybrid Screening—Yeast two-hybrid screening was performed using the Gal4-based Matchmaker two-hybrid system with the cDNA libraries derived from fetal human brain (first screening) and adult human brain (second screening) (Clontech, Palo Alto, CA). *Saccharomyces cerevisiae* CG1945 cells were transformed with pAS2–1-NEDL1-1 (amino acids 757–1114; first screening) or pAS2–1-NEDL1-2 (amino acids 382–1448; second screening), which did not activate the transcription of *lacZ* alone. The transformants were subsequently transformed with the cDNA library, and the *lacZ*-positive colonies were selected. The plasmid DNAs were extracted from these positive colonies, and their nucleotide sequences were determined.

Immunoprecipitation and Western Blot Analysis—Anti-NEDL1 and anti-TRAP-δ polyclonal antibodies were raised in rabbits against an NEDL1 oligopeptide (amino acids 460–482) and a TRAP-δ oligopeptide (amino acids 93–126), respectively. For immunoprecipitation, COS-7 or Neuro2a cells were cotransfected with the expression plasmids in various combinations and lysed 48 h later in 10 mM Tris-HCl (pH 7.8), 150 mM NaCl, 1% Nonidet P-40, 1 mM EDTA, and 1 mM phenylmethylsulfonyl fluoride supplemented with protease inhibitor mixture (Sigma). Whole cell lysates were immunoprecipitated with anti-NEDL1, anti-FLAG (M2; Sigma), or anti-Myc (9B11; Cell Signaling Technology, Beverly, MA) antibody. Immune complexes were recovered on protein G-Sepharose beads, eluted by boiling in Laemmli sample buffer, electrophoresed on SDS-polyacrylamide gel, and then transferred to a polyvinylidene difluoride membrane (Immobilon, Millipore Corp., Bedford, MA) by electroblotting. For ubiquitination experiments, cell lysis was performed in radioimmune precipitation assay buffer (10 mM Tris-HCl (pH 7.4), 150 mM NaCl, 1% Nonidet P-40, 0.1% sodium deoxycholate, 0.1% SDS, and 1 mM EDTA), followed by strong sonication and freeze-thaw. The membrane was probed with the indicated primary antibodies and then incubated with the appropriate secondary antibodies labeled with horseradish peroxidase (Jackson ImmunoResearch Laboratories, Inc. and Southern Biotechnology Associates, Inc., Birmingham, AL). Immunoreactive bands were detected by the enhanced chemiluminescence technique (ECL, Amersham Biosciences). For the detection of c-Jun phosphorylation, we used anti-c-Jun (sc-45, Santa Cruz Biotechnology, Santa Cruz, CA) or anti-phospho-Ser^{63} c-Jun (Cell Signaling Technology) antibody.

Cloning of Human NEDL1 cDNA—A forward primer (5′-GGTTTTTAGGCCTGGCCGCC-3′) and a reverse primer (5′-CAATGAGGTACATGCCAATCC-3′) were used to amplify the 5′-part of the *NEDL1* cDNA using cDNA libraries derived from human neuroblastoma and fetal human brain (Stratagene, La Jolla, CA) as templates. The full-length human *NEDL1* cDNA was generated by fusion of the PCR-amplified fragment (nucleotides +1 to +68, where position +1 represents the translation initiation site) and the *KIAA0322* cDNA (a gift from T. Nagase, Kazusa DNA Institute). Gel electrophoresis and Western blot analysis were carried out as described above.

Expression Constructs—The mammalian expression plasmids for hemagglutinin-tagged and His_6-tagged ubiquitin were kind gifts of D. Bohmann. The full-length *NEDL1* cDNA was inserted into the mammalian expression plasmid pEF1/His (Invitrogen) or pIRESpuro2 (Clontech). cDNAs encoding wild-type and mutant forms of SOD1 were fused to the FLAG or Myc epitope tag sequence at their C termini and subcloned into pIRESpuro2. Similarly, the FLAG or Myc epitope tag sequence was attached to the C terminus of TRAP-δ. Also similarly, the FLAG or Myc epitope tag sequence was attached to the N terminus of Dvl1. Coding sequences were verified by automated DNA sequencing.

Protein Stability Experiments—Neuro2a cells were transfected with the expression plasmid for the wild-type or mutant form of SOD1 with or without the NEDL1 expression plasmid. Twenty-four hours after transfection, cycloheximide (50 μg/ml) was added to the culture medium, and the cells were harvested at the indicated time points by lysis in radioimmune precipitation assay buffer. The protein concentrations were determined using the Bradford protein assay system (Bio-Rad) according to the instructions of the manufacturer.

Immunohistochemistry—The immunohistochemical studies were performed as described previously using affinity-purified rabbit anti-NEDL1 antibody (11). Patient tissues were obtained at autopsy from two FALS siblings from a Japanese family. The clinical course of the sister, who died at age 46, was 18 months (case 1), and that of the brother, who died at age 65, was 11 years (case 2) (11). The *SOD1* gene was mutated with a 2-bp deletion at codon 126 (11, 12). Normal spinal cord tissues were obtained from three neurologically and neuropathologically normal individuals. The same study was performed on spinal cord tissues from three normal rats and a transgenic ALS rat carrying a mutant allele of the human *SOD1* gene (H46R) (13). These mice were killed at 180 days. As a negative control, some sections were incubated with anti-NEDL1 antibody that had been pre-absorbed with an excess of NEDL1 antigen. Bound antibodies were visualized by the avidin-biotin-immunoperoxidase complex method.

RESULTS

Cloning and Expression of the NEDL1 E3 Gene—To detect novel molecules that are important in regulating neuronal programmed cell death, we constructed oligo-capping cDNA libraries from a mixture of three fresh human neuroblastoma tissues (stages 1 and 2) that were undergoing gradual spontaneous regression, probably by neuronal apoptosis (14). Screening of 1152 novel genes by RT-PCR revealed that 194 genes were expressed differentially in regressing neuroblastomas with favorable prognosis and in aggressive tumors with poor prognosis. Among these genes, we found a partial cDNA sequence with an HECT-like domain (*Nbla0078*) that partially matched the *KIAA0322* gene. Because *KIAA0322* lacks a 5′-coding region, we used a genome-based PCR procedure to clone the corresponding full-length cDNA. This is predicted to encode a protein product of 1585 amino acids with homology to NEDD4 E3 (15, 16), which includes a C2 domain at the N-terminal region supposed to mediate its membrane localization in a calcium-dependent manner, two WW motifs important for protein-protein interaction through binding to specific proline-rich clusters, and a conserved catalytic HECT domain at the C terminus (Fig. 1A). We named this novel ligase, which mapped to chromosome 7p13, NEDL1 (NEDD4-like ubiquitin-protein ligase-1). We also cloned the mouse counterpart of *NEDL1* cDNA, whose amino acid sequence is 78% identical to the human sequence. Tissue-specific expression of *NEDL1* mRNA of ~10 and 7 kb in size was observed, with predominant expression in adult and fetal brains as examined by Northern blot analysis (Fig. 1*B*). Its

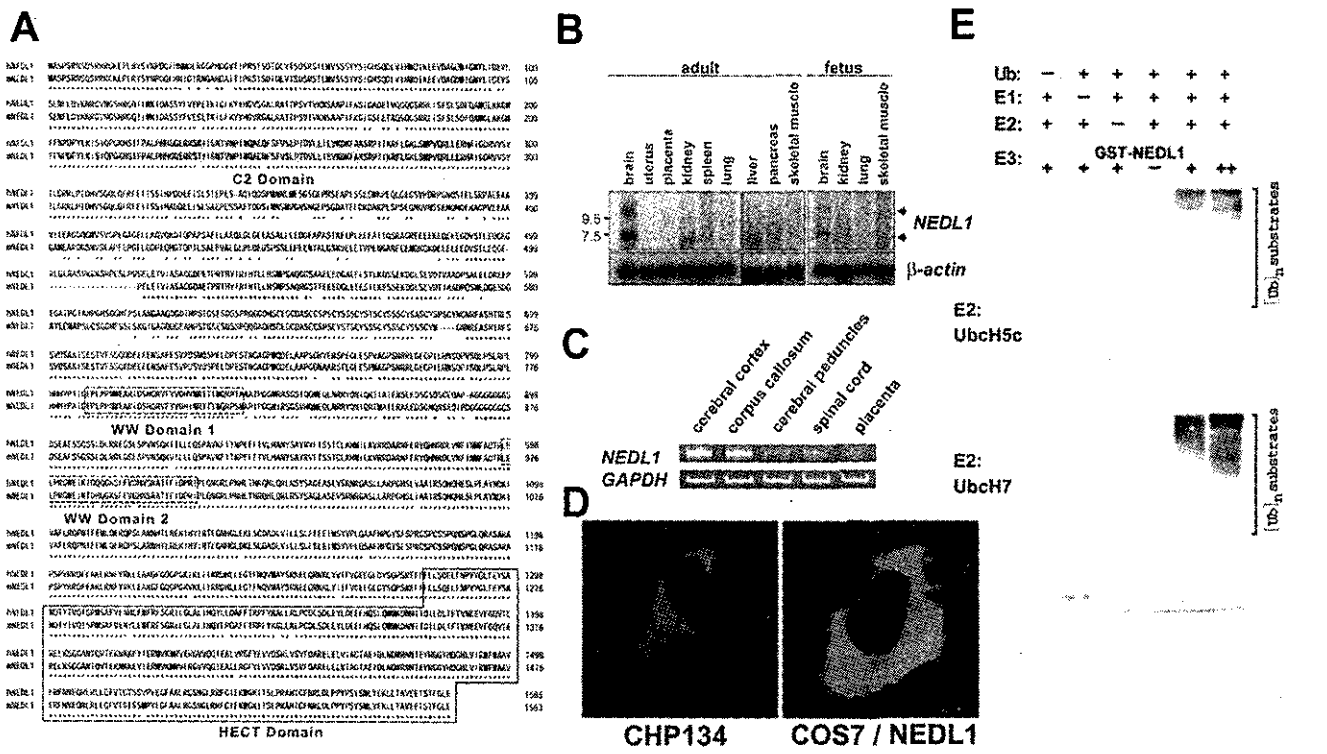

FIG. 1. **Amino acid sequence, brain-specific expression, and subcellular localization of NEDL1 E3.** *A*, alignment of conserved amino acid sequences of human NEDL1 (*hNEDL1*) and its mouse homolog (*mNEDL1*). *Numbers* on the right indicate the number of residues to the initiator methionine. The C2 domain (*shaded*), two WW domains (*dashed boxes*), and the HECT domain (*solid box*) are indicated. *B*, brain-specific expression of *NEDL1* mRNA. Total RNAs derived from the indicated adult (*left panel*) and fetal (*right panel*) human tissues were analyzed by Northern blotting using a ^{32}P-labeled human *NEDL1* cDNA restriction fragment as a probe. Control hybridization with a human β-actin cDNA probe verified the equal amount of RNA loaded. *C*, expression of *NEDL1* in human brain subsections. Total RNA from the cerebral cortex, corpus callosum, cerebral peduncles, spinal cord, or placenta was subjected to RT-PCR using specific primers for *NEDL1* or glyceraldehyde-3-phosphate dehydrogenase (*GAPDH*). RT-PCR analysis for *NEDL1* in the placenta provided a negative control. Amplification of glyceraldehyde-3-phosphate dehydrogenase was used as an internal control. *D*, confocal microscopic images of human neuroblastoma CHP134 cells (*left panel*) and COS-7 cells transfected with an expression plasmid for NEDL1 (*right panel*). Cells were subjected to immunofluorescence analysis using rabbit anti-NEDL1 polyclonal antibody, followed by fluorescein isothiocyanate-conjugated anti-mouse IgG. *E*, *in vitro* ubiquitination assays showing that NEDL1 has a ubiquitin-protein ligase activity. The degree of ubiquitination was increased in an NEDL1-dependent manner. In this assay, yeast ubiquitin-activating enzyme (*E1*), bacterially expressed ubiquitin carrier protein (*E2*; UbcH5C or UbcH7), and bacterial lysates were incubated in the presence or absence of increasing amounts of glutathione *S*-transferase (*GST*)-NEDL1. Polyubiquitinated bacterial proteins appeared to migrate in a high molecular mass complex. *Ub*, ubiquitin.

expression was also weakly detected in adult kidney, where the size of the expressed transcript appeared to be <7 kb. Expression of *NEDL1* in specific regions of the nervous system was further confirmed in the cerebral cortex, corpus callosum, cerebral peduncles, and spinal cord by RT-PCR (Fig. 1*C*). Thus, NEDL1 is a novel HECT-type E3 preferentially expressed in neuronal tissues, including the spinal cord. Using a specific anti-NEDL1 polyclonal antibody that we generated, we localized NEDL1 primarily to the cytoplasm in both intact human neuroblastoma CHP134 cells and COS-7 cells transiently expressing NEDL1 (Fig. 1*D*). The *in vitro* system containing UbcH5c or UbcH7 demonstrated that NEDL1 has a ubiquitin-protein ligase activity (Fig. 1*E*).

NEDL1 Physically Interacts with TRAP-δ and Mutant SOD1—We then sought protein-binding partners of NEDL1 by yeast two-hybrid screening using the region including two WW protein interaction domains (amino acids 757–1114) as bait. Of 96 positive clones subjected to DNA sequencing, one was a full-length cDNA for TRAP-δ; this was of considerable interest, as TRAP-δ was previously reported to bind mutant (G85R and G93A), but not wild-type, SOD1 (9). TRAP-δ is a protein component of the translocon in the ER membrane (10). We therefore examined the interaction among NEDL1, TRAP-δ, and SOD1 by an immunoprecipitation assay after cotransfecting the corresponding expression constructs into COS-7 cells. As shown in Fig. 2 (*A* and *B*), NEDL1 was physically associated with both exogenous and endogenous TRAP-δ probably through the region of two WW domains, as originally suggested by the result of two-hybrid screening. Surprisingly, NEDL1 bound to mutant (but not wild-type) SOD1 (Fig. 2*C*). Furthermore, the degree of binding between NEDL1 and different mutant SOD1 proteins was roughly proportionate to the rapidity of progression (time from clinical onset to death) of the associated FALS phenotype (17–23). For example, two mutant SOD1 proteins associated with an extremely rapid clinical course (C6F and A4V) interacted very strongly with NEDL1. By contrast, the binding of NEDL1 to other mutants was less striking and decreased proportionately to the falloff of disease severity corresponding to those mutants. Of further interest, like the NEDL1-mutant SOD1 interaction, the binding intensity between TRAP-δ and mutant SOD1 was also dependent on the disease severity (Fig. 2*D*). These observations suggest that NEDL1 and TRAP-δ are normally associated with each other, but that misfolded mutant SOD1 makes a complex with them. Such a complex is not formed with wild-type SOD1. The experiments using the *in vitro* translated proteins suggested that association of mutant SOD1 and TRAP-δ was direct (data not shown). It therefore appears that mutant SOD1 forms tightly bound protein complexes with NEDL1 and TRAP-δ and that the tightness of binding in the complex is determined in part by

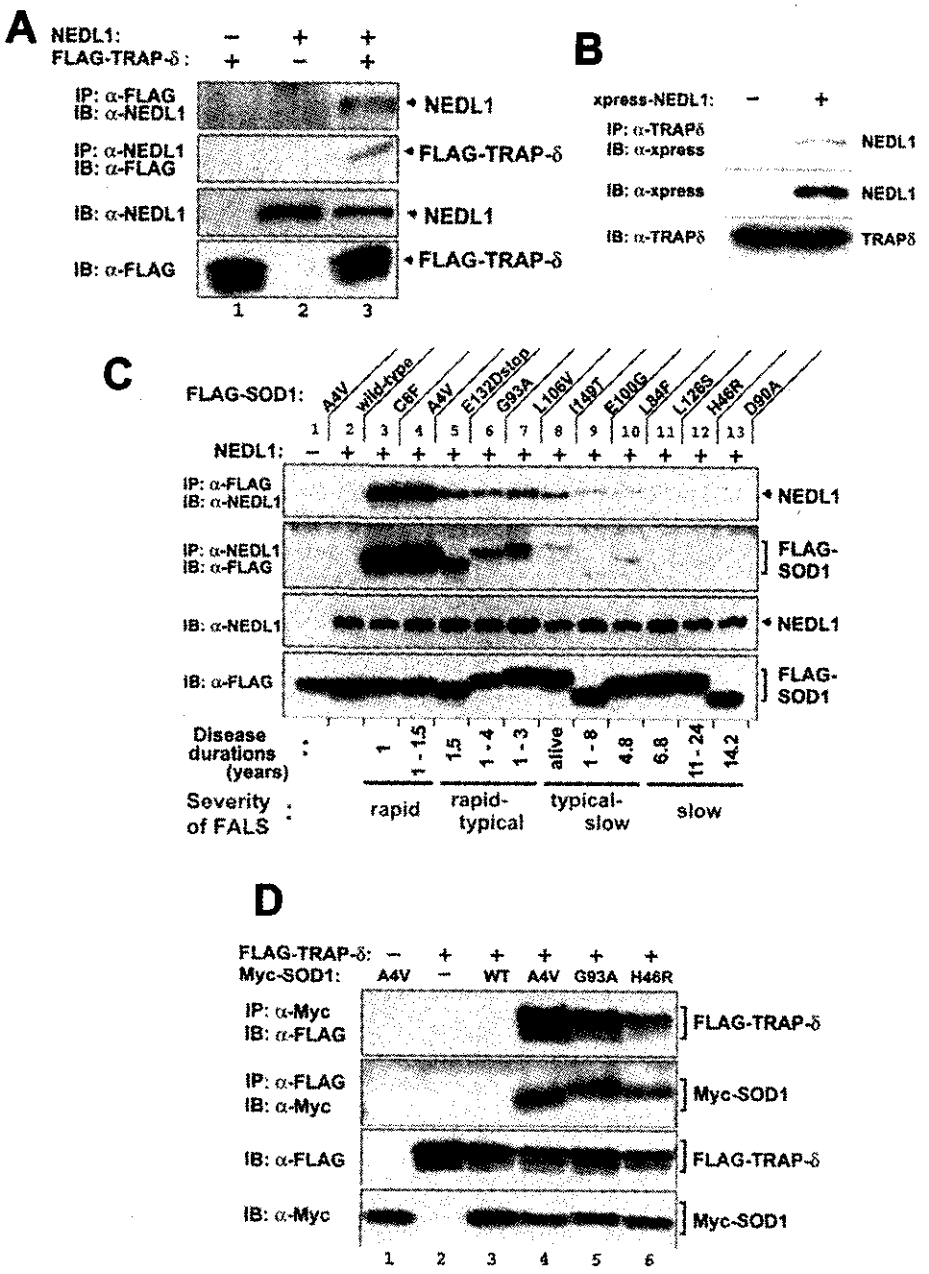

FIG. 2. **NEDL1 interacts with TRAP-δ and FALS-associated mutant forms of SOD1, but not with wild-type SOD1.** *A*, NEDL1 interacts with TRAP-δ. COS-7 cells were cotransfected with the indicated expression plasmids, and whole cell lysates were immunoprecipitated (*IP*) with anti-FLAG (*first panel*) or anti-NEDL1 (*second panel*) antibody. Immunoprecipitates were analyzed by immunoblotting (*IB*) using the indicated antibodies. Whole cell lysates were analyzed for expression levels of each protein by immunoblot analysis (*third* and *fourth panels*). Detection was performed with horseradish peroxidase-conjugated secondary antibodies. *B*, NEDL1 also binds to endogenous TRAP-δ. *C*, interaction between NEDL1 and mutant SOD1. Whole cell lysates from COS-7 cells overexpressing NEDL1 and one of the FLAG-tagged SOD1 mutants or wild-type SOD1 were immunoprecipitated with anti-FLAG (*first panel*) or anti-NEDL1 (*second panel*) antibody and then immunoblotted with anti-NEDL1 or anti-FLAG antibody, respectively. The expression of NEDL1 or FLAG-tagged SOD1 mutants was analyzed by immunoblotting using anti-NEDL1 (*third panel*) or anti-FLAG (*fourth panel*) antibody, respectively. Patients carrying the SOD1(C6F) and SOD1(A4V) mutations have a rapid clinical course, whereas mutant SOD1(L126S), SOD1(H46R), or SOD1(D90A) is associated with a slow clinical course. *D*, interaction of TRAP-δ with mutant SOD1. COS-7 cells were transiently cotransfected with the expression plasmid for FLAG-tagged TRAP-δ and the expression plasmid encoding one of the Myc-tagged SOD1 mutants or wild-type (*WT*) SOD1. Whole cell lysates were immunoprecipitated with anti-Myc (*first panel*) or anti-FLAG (*second panel*) antibody, followed by immunoblotting with anti-FLAG or anti-Myc antibody, respectively. The levels of overexpression of FLAG-tagged TRAP-δ (*third panel*) and Myc-tagged SOD1 (*fourth panel*) were analyzed by immunoblotting using anti-FLAG and anti-Myc antibodies, respectively.

properties of the mutant enzyme that also modulate disease severity of the resulting ALS phenotype. Such complexes do not form in cells with wild-type SOD1.

Determination of the Interaction Domains—We next examined the domains of NEDL1 required for formation of the SOD1·NEDL1·TRAP-δ complex. We generated various constructs of NEDL1 with deletions of each domain. Fig. 3 shows the results of immunoprecipitation assay for the association between deletion mutants of NEDL1 and mutant SOD1(G93A). Mutant SOD1 bound weakly to NEDL1 lacking WW domain-1 (Fig. 3*A*), suggesting that WW domain-1 and its surrounding portion are the region involved in their interaction. Immuno-

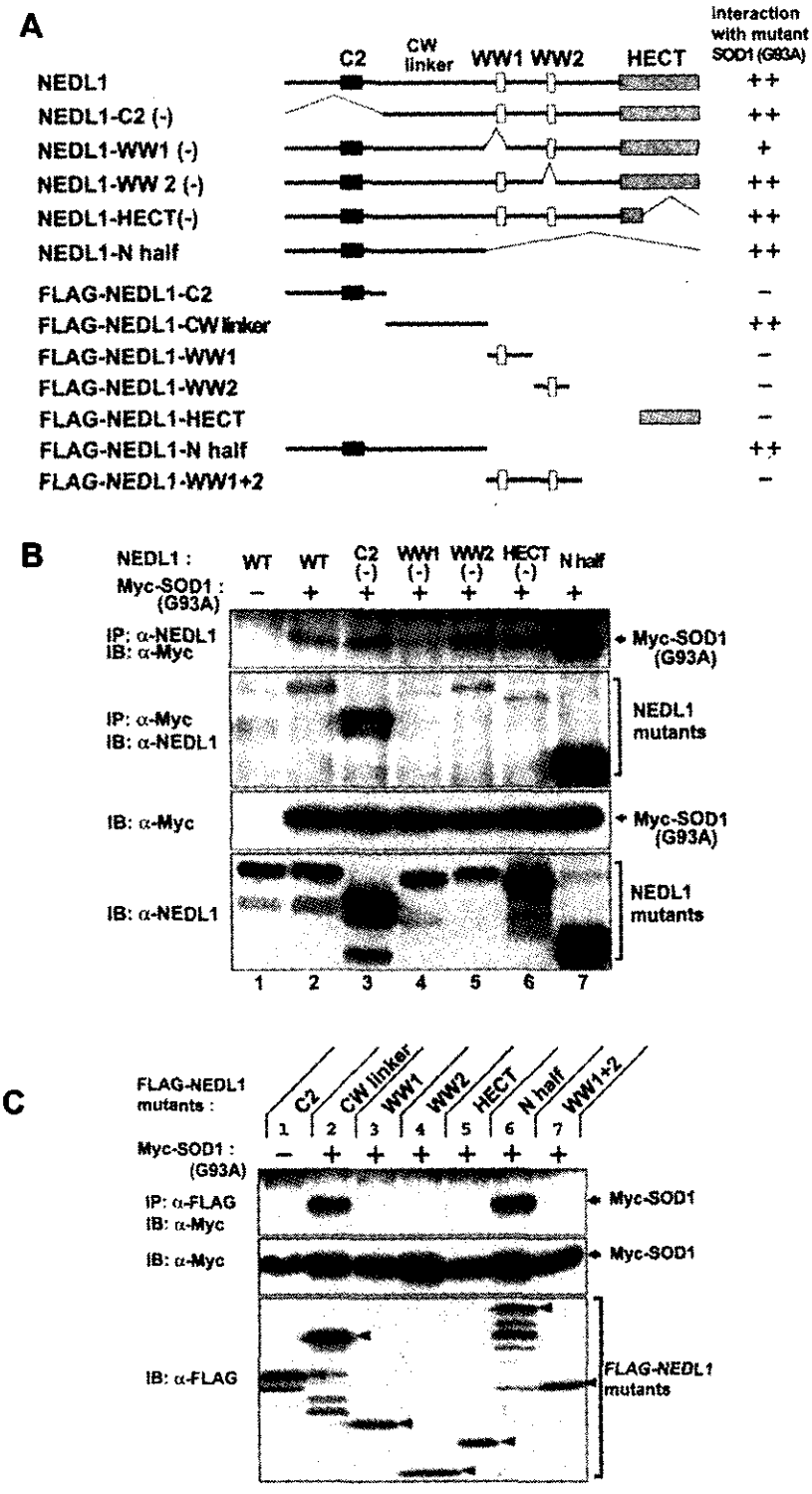

FIG. 3. **The region of NEDL1 between the C2 domain and WW domain-1 is required for interaction with mutant SOD1.** *A*, schematic illustration of wild-type NEDL1 and a series of deletion mutants of NEDL1. *CW linker* indicates the region between the C2 domain and WW domain-1 (*WW1*). *B* and *C*, immunoprecipitation and immunoblot analyses. In *B*, Myc-tagged mutant SOD1(G93A) was overexpressed together with wild-type (*WT*) NEDL1 or the indicated deletion mutants of NEDL1 in COS-7 cells. Whole cell lysates were immunoprecipitated (*IP*) with anti-NEDL1 (*first panel*) or anti-Myc (*second panel*) antibody, followed by immunoblotting (*IB*) with anti-Myc or anti-NEDL1 antibody, respectively. The expression levels of each protein were analyzed by immunoblotting using the indicated antibodies (*third* and *fourth panels*). In *C*, whole cell lysates were immunoprecipitated with anti-FLAG antibody and then immunoblotted with anti-Myc antibody (*upper panel*). Whole lysates were also analyzed by Western blotting for each protein (*middle* and *lower panels*).

precipitation analysis using the specific regions of NEDL1 clearly showed that the region between the C2 domain and WW domain-1 (CW linker region) is necessary for binding to mutant SOD1(G93A). Mutant SOD1(A4V) was also associated with NEDL1 through the same region, and TRAP-δ bound to the two WW domains of NEDL1 (data not shown).

NEDL1 Ubiquitinates Mutant SOD1 for Degradation Depending on the Disease Severity of FALS—Because NEDL1 is an E3, we next tested whether it ubiquitinates TRAP-δ and mutant SOD1 for degradation. As shown in Fig. 4*A*, NEDL1 clearly ubiquitinated mutant SOD1(A4V), but not TRAP-δ (data not shown). Furthermore, the degree of ubiquitination of mutant SOD1 by NEDL1 was dependent on the disease severity of FALS (A4V > G93A > H46R) (Fig. 4*A*). Fig. 4*B* shows the time course of degradation of wild-type and mutant SOD1 in the presence or absence of NEDL1. As reported previously (46), mutant SOD1 was degraded more rapidly than wild-type SOD1. NEDL1 did not affect wild-type SOD1 degradation. As expected from the co-immunoprecipitation and ubiquitination analyses, degradation of mutant SOD1 was stimulated by NEDL1 proportionately to the disease severity of FALS caused by the particular SOD1 mutant (A4V > G93A > H46R ≥

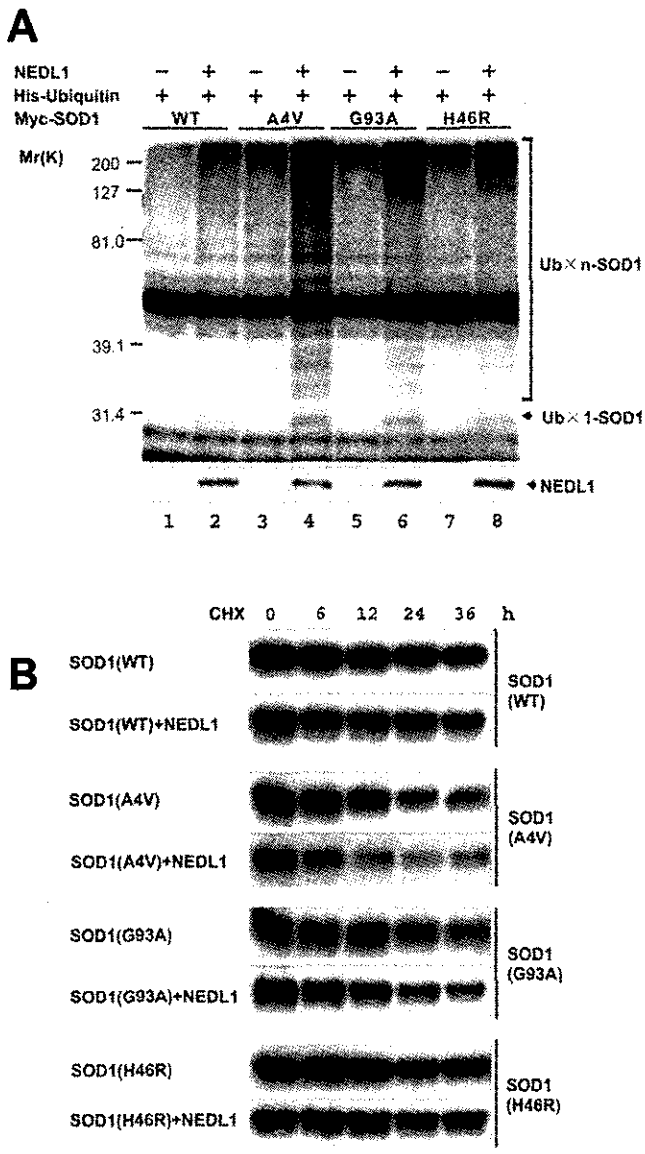

FIG. 4. **NEDL1-dependent ubiquitination and degradation of mutant forms of SOD1 correlate broadly with their respective clinical phenotypes.** *A*, NEDL1 ubiquitinates mutant SOD1 in a mutant type-dependent manner. COS-7 cells were transiently cotransfected with the indicated expression plasmids. Whole cell lysates from transfected COS-7 cells were immunoprecipitated with anti-Myc antibody, and immunoprecipitates were analyzed by Western blotting with anti-ubiquitin (*Ub*) antibody (*upper panel*). The *bracket* indicates slowly migrating ubiquitinated forms of SOD1. Whole cell lysates were analyzed by immunoblotting with anti-NEDL1 antibody to confirm the expression of transfected NEDL1 (*lower panel*). The running positions of molecular weight markers are indicated on the left. *B*, half-lives of wild-type (*WT*) and mutant SOD1 proteins in the presence or absence of NEDL1. Cell lysates were harvested from Neuro2a cells transfected with *SOD1* alone or with *SOD1* plus *NEDL1* at different time points as indicated after the addition of cycloheximide (*CHX*; final concentration of 50 μg/ml) and were analyzed for SOD1 protein levels by Western blotting with anti-FLAG antibody. In the presence of NEDL1, the half-lives of various mutant SOD1 proteins were reduced also roughly dependent on the disease severity of FALS (A4V > G93A > H46R).

wild-type). Thus, NEDL1 targeted mutant SOD1 for ubiquitin-mediated degradation in the cell in parallel with the binding intensity.

Immunohistochemistry—One of the characteristic cytopathological changes of mutant SOD1-linked FALS is the formation of neuronal Lewy body-like hyaline inclusions (LBHIs) that contain aggregates of SOD1 and ubiquitin (24). We therefore

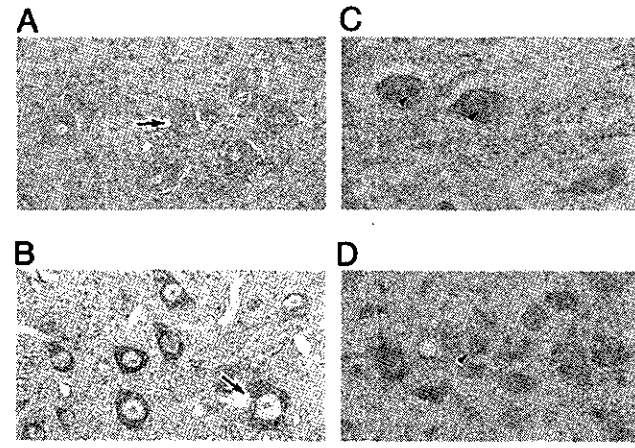

FIG. 5. **NEDL1 immunohistochemical analyses.** *A*, immunohistochemical analysis of NEDL1 in normal human spinal cord. NEDL1-positive anterior horn cells are evident (*arrow*), although the immunoreactivity for NEDL1 is somewhat faint. There was no counterstaining. Magnification ×520. *B*, NEDL1 immunohistochemistry in normal mouse spinal cord. Normal anterior horn cells are positive for NEDL1 (*arrow*). The section was counterstained with hematoxylin. Magnification ×750. *C*, immunostaining for NEDL1 in spinal cord LBHIs from an FALS patient with a frameshift 126 mutation in the *SOD1* gene. The NEDL1-positive reaction products were mostly restricted to the cores of the core and halo-type LBHIs (*arrowheads*). In the LBHI-bearing neurons and residual neurons, the antibody to NEDL1 also stained the neuronal cell body. There was no counterstaining. Magnification ×540. *D*, NEDL1 immunostaining in a spinal cord LBHI from an *SOD1*(H46R) transgenic mouse. An ill defined LBHI in the *SOD1*(H46R) transgenic mouse was positive for NEDL1; this ill defined LBHI shows a diffuse staining pattern (*arrowhead*). The staining intensity in the residual neurons stained by anti-NEDL1 antibody varied from neuron to neuron. The section was counterstained with hematoxylin. Magnification ×770.

performed immunostaining to determine whether the NEDL1 protein is included within the LBHIs of the spinal cord motor neurons obtained from two siblings with FALS caused by frameshift 126 mutation of SOD1 (11, 12). One case had neuropathological findings compatible with FALS with posterior column involvement, whereas the other had multisystem degeneration in addition to motor neuron disturbance. We also performed NEDL1 immunostaining in specimens obtained from mutant *SOD1*(H46R) transgenic mice at 180 days, by which time they show clinical motor signs in the hind limbs (13). The specificity of the NEDL1 staining was confirmed by pretreating the specimens with an excess of NEDL1 antigen. NEDL1 immunoreactivity in the spinal cords of the human control cases was identical to that of normal mice: immunoreactivity was identified predominantly in the cytoplasm of the neurons of the spinal cords (Fig. 5, *A* and *B*). The LBHIs in the anterior horn cells of two FALS patients and transgenic mice showed equivalent immunoreactivity for NEDL1. Although the intensity of NEDL1 immunoreactivity in neuronal LBHIs varied, most of the LBHIs were immunoreactive for NEDL1 (Fig. 5, C and *D*). The reaction products were generally restricted to the cores of the core and halo-type LBHIs that showed eosinophilic cores with pale peripheral halos upon hematoxylin and eosin staining (Fig. 5*C*); by contrast, immunopositive NEDL1 in ill defined LBHIs was distributed throughout the inclusions (Fig. 5*D*). NEDL1 immunoreactivity in the residual neurons in humans and mice was identified primarily in cell bodies. Thus, NEDL1 immunostaining was clearly positive in the FALS-related LBHIs that were also positive for ubiquitin and SOD1 (data not shown).

NEDL1 Targets Dishevelled-1 for Ubiquitin-mediated Protein Degradation—We next hypothesized that the physiological function of NEDL1 to mediate ubiquitination is interfered with

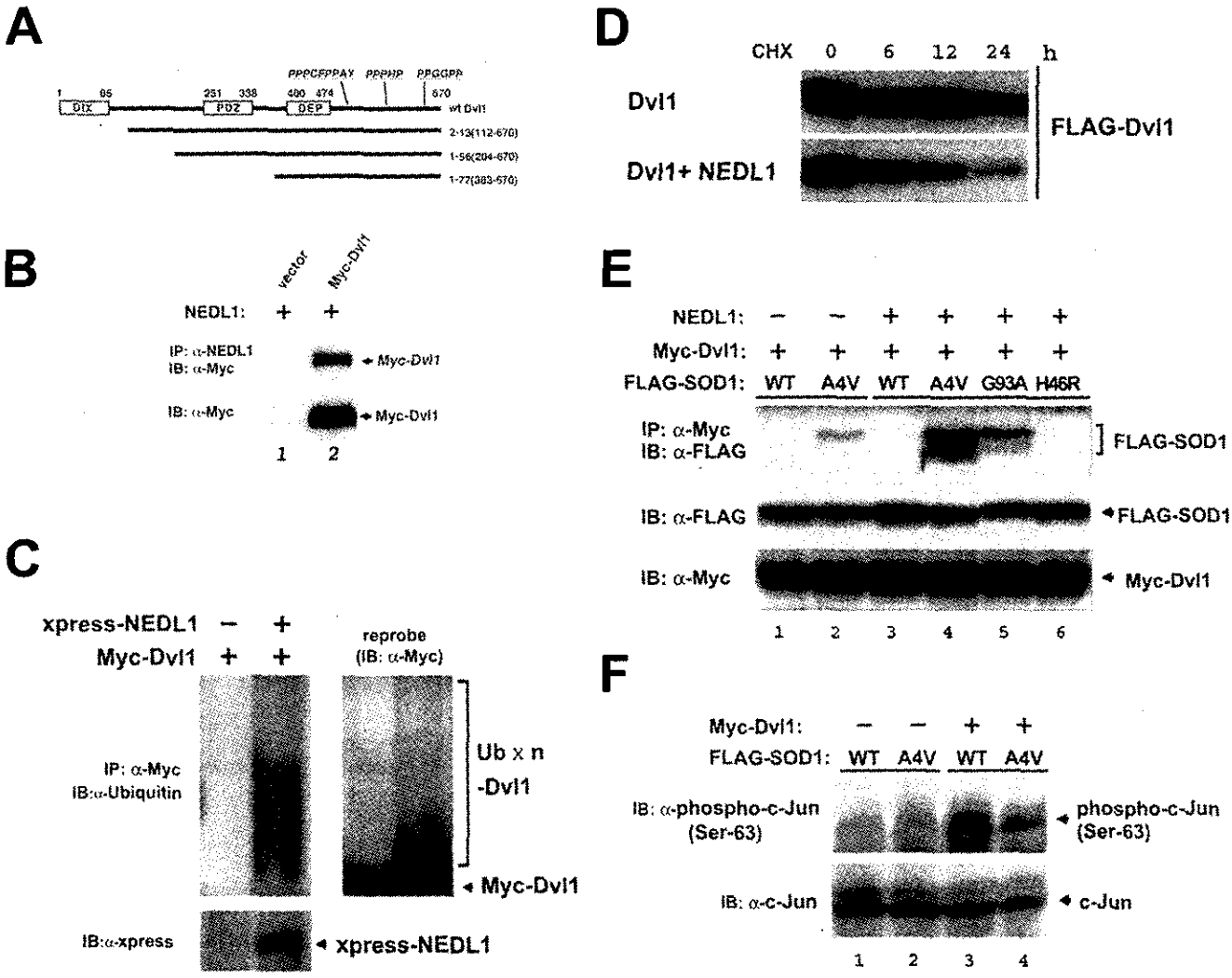

FIG. 6. **Dvl1 is a substrate of NEDL1, and its functions are disturbed by mutant SOD1(A4V).** *A*, schematic illustration of full-length Dvl1 and three clones obtained by yeast two-hybrid screening. Human Dvl1 consists of 670 amino acids and contains three conserved domains, including the DIX, PDZ, and DEP domains. Between the DEP domain and the C-terminal end, there are three proline-rich clusters, which might act as WW domain recognition sites. All three clones (clones 2–13, 1–56, 1–77) contain the DEP domain and these clusters. *B*, NEDL1 interacts with Dvl1. Myc-tagged Dvl1 was overexpressed together with NEDL1 in Neuro2a cells. Whole cell lysates were immunoprecipitated (*IP*) with anti-NEDL1 antibody, followed by immunoblotting (*IB*) with anti-Myc antibody (*upper panel*). The expression levels of Myc-tagged Dvl1 were analyzed by immunoblotting using anti-Myc antibody (*lower panel*). *C*, NEDL1 ubiquitinates Dvl1 in Neuro2a cells. The cells were transiently transfected with the indicated expression plasmids along with the ubiquitin expression plasmid in the presence or absence of the expression plasmid for XPRESS-tagged NEDL1. Whole cell lysates were immunoprecipitated with anti-Myc antibody and then immunoblotted with anti-ubiquitin antibody (*left panel*). The ladder of bands denoted by the *bracket* appeared to be ubiquitinated Dvl1. The expression of XPRESS-NEDL1 was analyzed by immunoblotting using anti-XPRESS antibody. The membrane was reprobed with anti-Myc antibody (*right panel*). *D*, Dvl1 is degraded by NEDL1. Neuro2a cells were transfected with the expression plasmid for FLAG-tagged Dvl1 with or without the NEDL1 expression plasmid. Transfected cells were harvested at different time points as indicated after the addition of cycloheximide (*CHX*; final concentration of 50 μg/ml), and Dvl1 protein levels were analyzed by Western blotting with anti-FLAG antibody. In the presence of NEDL1, the half-lives of FLAG-Dvl1 were significantly reduced. *E*, Dvl1 binds to mutant SOD1(A4V), and the degree of its binding is enhanced in the presence of NEDL1. Whole cell lysates prepared from COS-7 cells transfected with the indicated combinations of expression plasmids were subjected to immunoprecipitation and Western analyses as indicated. *F*, c-Jun phosphorylation by overexpression of Dvl1 is suppressed upon coexpression of mutant *SOD1(A4V)*. Whole cell lysates from COS-7 cells transfected with the indicated combinations of expression plasmids were subjected to Western blotting with antibody against the phosphorylated form of c-Jun (*upper panel*) or with anti-c-Jun antibody (*lower panel*). *wt/WT*, wild-type.

by mutant SOD1. To test this hypothesis, we again performed yeast two-hybrid screening to obtain NEDL1-interacting molecules using the large region of NEDL1 (amino acids 382–1448) as bait. Of 396 His and β-galactosidase double-positive clones, 282 clones were subjected to DNA sequencing, and we identified Dvl1 (three clones). Human Dvl1 is a 670-amino acid protein with three conserved domains: a DIX domain, which is required for canonical Wnt/T-cell factor signaling; a PDZ domain, which is a target of both Stbm and casein kinase I binding; and a DEP domain, which is responsible for Dvl membrane localization during planar cell polarity signaling (25–27). Between the DEP domain and C-terminal end, there are three proline-rich clusters unique to mammalian Dvl1, which presumably act as the WW domain recognition sites. All three clones (clones 2–13, 1–56, and 1–77) contain the DEP domain and proline-rich clusters, suggesting that NEDL1 interacted with Dvl1 in the C-terminal half (Fig. 6*A*). In Neuro2a cells, NEDL1 co-immunoprecipitated with Dvl1 (Fig. 6*B*) and ubiquitinated it for degradation (Fig. 6, *C* and *D*). Thus, Dvl1 may be one of the physiological targets of NEDL1 E3. As recent studies strongly suggest that the cytotoxicity of SOD1 mutants is responsible for their aggregate properties, incorporating other proteins essential for cells into their aggregates (28), we examined the association between mutant *SOD1* and Dvl1,

both of which interact with NEDL1. Of interest, Dvl1 bound to mutant SOD1(A4V), and complex formation was increased in the presence of NEDL1 roughly proportionately to the disease severity of FALS caused by the particular SOD1 mutant (Fig. 6*E*). Dvl1 is known to transduce not only the Wnt/β-catenin/T-cell factor pathway, but also the JNK/c-Jun pathway (27). Therefore, we next examined whether the Dvl1-induced phosphorylation of c-Jun at Ser^{63} was affected by the tight complex formation induced by inclusion of mutant SOD1. As shown in Fig. 6*F*, c-Jun phosphorylation induced by overexpression of Dvl1 was significantly suppressed by coexpression with mutant SOD1(A4V) in COS-7 cells.

DISCUSSION

Our present results demonstrate that a novel HECT-type NEDL1 E3, which is preferentially expressed in neuronal tissues, specifically targets mutant forms of SOD1 for ubiquitination-mediated protein degradation. NEDL1 is also associated with TRAP-δ localized at the ER translocon. The TRAP complex has recently been shown to facilitate the initiation of protein translocation in a substrate-specific manner (29). The NEDL1·TRAP-δ complex recognizes mutant (but not wild-type) SOD1, with a binding intensity that broadly parallels the disease severity of FALS. NEDL1 immunoreactivity was detected in the FALS-related LBHIs in the spinal cord ventral horn motor neurons, suggesting that, although mutant SOD1 is ubiquitinated for degradation by NEDL1, the mutant SOD1·NEDL1·TRAP-δ complex aggregates within the LBHIs. It is also conceivable that fragmentation of the Golgi apparatus reported in ALS patients and transgenic mice might be related to this aggregation (30, 31). These findings suggest possible hypotheses for the role of NEDL1 in the pathogenesis of FALS: 1) NEDL1, alone or with TRAP-δ, ubiquitinates and aggregates mutant SOD1, thereby decreasing the function of mutant SOD1; 2) NEDL1 and TRAP-δ form aggregates with mutant SOD1 that induce fragmentation of the Golgi apparatus, leading to neuronal apoptosis; 3) formation of these aggregates causes dysfunction of NEDL1 and/or TRAP-δ, and this, in turn, induces disturbances that ultimately cause motor neuron death; and 4) the mutant SOD1·NEDL1·TRAP-δ aggregates trap and inactivate unknown factor(s) such as molecular chaperones whose normal function is important for motor neuron viability.

To further understand the role of NEDL1 in motor neuron death, we searched for the physiological targets of NEDL1 and identified Dvl1. As expected, Dvl1 is ubiquitinated for degradation by NEDL1. Surprisingly, however, Dvl1 also interacts with mutant SOD1 in the presence of NEDL1 roughly proportionately to the disease severity of FALS caused by the particular SOD1 mutant. Dvl1, an essential multimodule signal transducer localized in the cellular cytosol and cytoskeleton, mediates planar cell polarity signaling as well as canonical Wnt/β-catenin signaling (27, 32). In mammals, three Dvl family members have so far been reported, and the level of Dvl1 expression is high in neuronal tissues (33). As far as we know, NEDL1 is the first E3 for Dvl1, interacting with the C-terminal region containing three proline-rich clusters. A recent report suggests that Dvl1 regulates microtubule stability through inhibition of glycogen synthase kinase-3β (34). Because cytoskeletal abnormalities have been reported in ALS motor neurons (35), it is possible that the effect of mutant SOD1 on NEDL1-mediated Dvl1 degradation is involved in the motor neuron death. Furthermore, Dvl1 is abundant in the postsynaptic membrane region at the neuromuscular junction (36) that is reported to be involved in several neurodegenerative disorders (37, 38). Of interest, *Dvl1* is mapped to chromosome 1p36, which is a commonly deleted region in many human cancers, including neuroblastoma (39). As NEDL1 is highly expressed in neuroblastomas with favorable prognosis, which have a tendency to differentiate and/or regress, NEDL1 may be involved in the regulation of neuronal differentiation and survival possibly by controlling Dvl1.

NEDL1, TRAP-δ, mutant SOD1, and Dvl1 appear to form a complex roughly proportionately to the disease severity of FALS caused by the particular SOD1 mutant. Our present observations strongly suggest that NEDL1 may be a quality control E3 recognizing misfolded mutant SOD1 (40). The association between mutant SOD1 and NEDL1 may induce the conformational change in the NEDL1 protein to increase the binding intensity with other physiological targets such as TRAP-δ (not ubiquitinated) and Dvl1 (ubiquitinated). This may lead to tight complex formation especially when the proteasome activity is impaired. It has been reported that the expression and function of proteasomes decrease with age in the spinal cord (7). Okado-Matsumoto and Fridovich (41) have also found that complex formation between mutant SOD1 and heat shock proteins leads to protein aggregates. Because our data show that the ER translocon component TRAP-δ is involved, aggregate formation may occur at the sites of the ER or Golgi apparatus or even at other cellular sites. The complex formation including NEDL1 and mutant SOD1 may conversely affect the physiological function of NEDL1, as demonstrated by a decrease in Dvl1-induced phosphorylation of c-Jun.

Recently, the RING finger-type E3 Dorfin has been reported to ubiquitinate mutant SOD1 for degradation (42). However, NEDL1 and Dorfin appear to be different in several aspects. First, NEDL1 is expressed specifically in neuronal tissues, including the spinal cord, whereas Dorfin is ubiquitously expressed in most human tissues. Second, both interaction between NEDL1 and mutant SOD1 and ubiquitination of the latter by NEDL1 roughly parallel the disease severity caused by the particular SOD1 mutant, whereas Dorfin similarly ubiquitinates mutant forms of SOD1. In addition, we have identified Dvl1 and TRAP-δ as cellular target proteins of NEDL1, whereas the physiological targets of Dorfin have never been reported. It is probable that there are some other E3 ligases targeting mutant SOD1. However, the molecular characteristics, including tissue-specific expression, subcellular localization, and age-dependent expression, might be important in the development of the FALS phenotype.

In conclusion, we have identified a novel neuronal E3 (NEDL1) that interacts with TRAP-δ and also binds to and ubiquitinates Dvl1 for degradation. Strikingly, NEDL1 targets and ubiquitinates mutant (but not wild-type) SOD1 for degradation. NEDL1 may normally function in the quality control of cellular proteins by eliminating misfolded proteins such as mutant SOD1, possibly via a mechanism analogous to that of ER-associated degradation (43–45). NEDL1 appears to complex tightly with mutant SOD1, Dvl1, and TRAP-δ, forming aggregates with species of mutant SOD1 that have escaped ubiquitin-mediated degradation. The NEDL1 function that affects the activities of the target proteins may also be modulated by mutant SOD1. All of these might contribute to the pathogenesis of FALS; further elucidation of the molecular mechanism of formation of this complex and its pathogenicity may provide insights into motor neuron death in ALS as well as possible new therapeutic strategies for ALS.

Acknowledgments—We thank Robert H. Brown, Jr. (Harvard Medical School) for critical comments and reading the manuscript. We also thank M. Ohira and Y. Nakamura for helping with cDNA cloning and sequencing; K. Watanabe and M. Suzuki for making plasmid constructs; M. Nagai and M. Kato for helping with immunohistochemical studies; S. Hatakeyama, M. Matsumoto, and K. Nakayama

for ubiquitination assay instruction; and S. Sakiyama for reading the manuscript.

REFERENCES

1. Rosen, D. R., Siddique, T., Patterson, D., Figlewicz, D. A., Sapp, P., Hentati, A., Donaldson, D., Goto, J., O'Regan, J. P., Deng, H. X., Rahmani, Z., Krizus, A., McKenna-Yasek, D., Cayabyab, A., Gaston, S. M., Berger, R., Tanzi, R. E., Halperin, J. J., Herzfeldt, B., van den Bergh, R., Hung, W.-Y., Bird, T., Deng, G., Mulder, D. W., Smyth, C., Laing, N. G., Soriano, E., Pericak-Vance, M. A., Haines, J., Rouleau, G. A., Gusella, J. S., Horvitz, H. R., and Brown, R. H., Jr. (1993) *Nature* **364,** 59–62
2. Deng, H. X., Hentati, A., Tainer, J. A., Iqbal, Z., Cayabyab, A., Hung, W.-Y., Getzoff, E. D., Hu, P., Herzfeldt, B., Roos, R. P., Warner, C., Deng, G., Soriano, E., Smyth, C., Parge, H. E., Ahmed, A., Roses, A. D., Hallewell, R., Rericak-Vance, M. A., and Siddique, T. (1993) *Science* **261,** 1047–1051
3. Cleveland, D. W., and Liu, J. (2001) *Nat. Med.* **6,** 1320–1321
4. Brown, R. H., Jr., and Robberecht, W. (2001) *Semin. Neurol.* **21,** 131–139
5. Cluskey, S., and Ramsden, D. B. (2001) *Mol. Pathol.* **54,** 386–392
6. Orrell, R. W., and Figlewicz, D. A. (2001) *Neurology* **57,** 9–17
7. Keller, J. N., Huang, F. F., and Markesbery, W. R. (2000) *Neuroscience* **98,** 149–156
8. Hoffman, E. K., Wilcox, H. M., Scott, R. W., and Siman, R. (1996) *J. Neurol. Sci.* **139,** 15–20
9. Kunst, C. B., Mezey, E., Brownstein, M. J., and Patterson, D. (1997) *Nat. Genet.* **15,** 91–94
10. Hartmann, E., Gorlich, D., Kostka, S., Otto, A., Kraft, R., Knespel, S., Burger, E., Rapoport, T. A., and Prehn, S. (1993) *Eur. J. Biochem.* **214,** 375–381
11. Kato, S., Shimoda, M., Watanabe, Y., Nakashima, K., Takahashi, K., and Ohama, E. (1996) *J. Neuropathol. Exp. Neurol.* **55,** 1089–1101
12. Kato, S., Hayashi, H., Nakashima, K., Nanba, E., Kato, M., Hirano, A., Nakano, I., Asayama, K., and Ohama, E. (1997) *Am. J. Pathol.* **151,** 611–620
13. Nagai, M., Aoki, M., Miyoshi, I., Kato, M., Pasinelli, P., Kasai, N., Brown, R. H., Jr., and Itoyama, Y. (2001) *J. Neurosci.* **21,** 9246–9254
14. Nakagawara, A. (1998) *Med. Pediatr. Oncol.* **31,** 113–115
15. Harvey, K. F., and Kumar, S. (1999) *Trends Cell Biol.* **9,** 166–169
16. Kumar, S., Tomooka, Y., and Noda, M. (1992) *Biochem. Biophys. Res. Commun.* **30,** 1155–1161
17. Kato, S., Takikawa, M., Nakashima, K., Hirano, A., Cleveland, D. W., Kusaka, H., Shibata, N., Kato, M., Nakano, I., and Ohama, E. (2000) *Amyotroph. Lateral Scler. Other Motor Neuron Disord.* **1,** 163–184
18. Orrell, R. W. (2000) *Neuromuscul. Disord.* **10,** 63–68
19. Cudkowicz, M. E., McKenna-Yasek, D., Sapp, P. E., Chin, W., Geller, B., Hayden, D. L., Schoenfeld, D. A., Hosler, B. A., Horvitz, H. R., and Brown, R. H., Jr. (1997) *Ann. Neurol.* **41,** 210–221
20. Ratovitski, T., Corson, L. B., Strain, J., Wong, P., Cleveland, D. W., Culotta, V. C., and Borchelt, D. R. (1999) *Hum. Mol. Genet.* **8,** 1451–1460
21. Aoki, M., Ogasawara, M., Matsubara, Y., Narisawa, K., Nakamura, S., Itoyama, Y., and Abe, K. (1993) *Nat. Genet.* **5,** 323–324
22. Kato, M., Aoki, M., Ohta, M., Nagai, M., Ishizaki, F., Nakamura, S., and Itoyama, Y. (2001) *Neurosci. Lett.* **312,** 165–168
23. Andersen, P. M., Forsgren, L., Binzer, M., Nilsson, P., Ala-Hurula, V., Keranen, M. L., Bergmark, L., Saarinen, A., Haltia, T., Tarvainen, I., Kinnunen, E., Udd, B., and Marklund, S. L. (1996) *Brain* **119,** 1153–1172
24. Shibata, N., Hirano, A., Kobayashi, M., Siddique, T., Deng, H. X., Hung, W.-Y., Kato, T., and Asayama, K. (1996) *J. Neuropathol. Exp. Neurol.* **55,** 481–490
25. Sussman, D. J., Klingensmith, J., Salinas, P., Adams, P. S., Nusse, R., and Perrimon, N. (1994) *Dev. Biol.* **166,** 73–86
26. Wodarz, A., and Nusse, R. (1998) *Annu. Rev. Cell Dev. Biol.* **14,** 59–88
27. Boutros, M., Paricio, N., Strutt, D. I., and Mlodzik, M. (1998) *Cell* **94,** 109–118
28. Julien, J. P. (2001) *Cell* **104,** 581–591
29. Fons, R. D., Bogert, B. A., and Hegde, R. S. (2003) *J. Cell Biol.* **160,** 529–539
30. Fujita, Y., Okamoto, K., Sakurai, A., Gonatas, N. K., and Hirano, A. (2000) *J. Neurol. Sci.* **174,** 137–140
31. Mourelatos, Z., Gonatas, N. K., Stieber, A., Gurney, M. E., and Dal Canto, M. C. (1996) *Proc. Natl. Acad. Sci. U. S. A.* **93,** 5472–5477
32. Wharton, K. A., Jr. (2003) *Dev. Biol.* **253,** 1–17
33. Tsang, M., Lijam, N., Yang, Y., Beier, D. R., Wynshaw-Boris, A., and Sussman, D. J. (1996) *Dev. Dyn.* **207,** 253–262
34. Krylova, O., Messenger, M. J., and Salinas, P. C. (2000) *J. Cell Biol.* **151,** 83–94
35. Julien, J. P., and Beaulieu, J. M. (2000) *J. Neurol. Sci.* **180,** 7–14
36. Luo, Z. G., Wang, Q., Zhou, J. Z., Wang, J., Luo, Z., Liu, M., He, X., Wynshaw-Boris, A., Xiong, W. C., Lu, B., and Mei, L. (2002) *Neuron* **35,** 489–505
37. De Ferrari, G. V., and Inestrosa, N. C. (2000) *Brain Res. Brain Res. Rev.* **33,** 1–12
38. Kaytor, M. D., and Orr, H. T. (2000) *Curr. Opin. Neurobiol.* **12,** 275–278
39. Versteeg, R., Caron, H., Cheng, N. C., van der Drift, P., Slater, R., Westerveld, A., Voute, P. A., Delattre, O., Laureys, G., van Roy, N., and Speleman, F. (1995) *Eur. J. Cancer* **31,** 538–541
40. Murata, S., Minami, Y., Minami, M., Chiba, T., and Tanaka, K. (2001) *EMBO Rep.* **2,** 1133–1138
41. Okado-Matsumoto, A., and Fridovich, I. (2002) *Proc. Natl. Acad. Sci. U. S. A.* **99,** 9010–9014
42. Niwa, J., Ishigaki, S., Hishikawa, N., Yamamoto, M., Doyu, M., Murata, S., Tanaka, K., Taniguchi, N., and Sobue, G. (2002) *J. Biol. Chem.* **277,** 36793–36798
43. Mori, K. (2000) *Cell* **101,** 451–454
44. Travers, K. J., Patil, C. K., Wodicka, L., Lockhart, D. J., Weissman, J. S., and Walter, P. (2000) *Cell* **101,** 249–258
45. Wickner, S., Maurizi, M. R., and Gottesman, S. (1999) *Science* **286,** 1888–1893
46. Borchelt, D. R., Lee, M. K., Slunt, H. S., Guarnieri, M., Xu, Z. S., Wong, P. C., Brown, R. H., Jr., Price, D. L., Sisodia, S. S., and Cleveland, D. W. (1994) *Proc. Natl. Acad. Sci. U. S. A.* **16,** 8292–8296

Available online at www.sciencedirect.com
SCIENCE DIRECT®
Cancer Letters 204 (2004) 213–224
CANCER Letters
www.elsevier.com/locate/canlet

Comprehensive genomics linking between neural development and cancer: neuroblastoma as a model

Akira Nakagawara*, Miki Ohira

Division of Biochemistry, Chiba Cancer Center Research Institute, 666-2 Nitona, Chuoh-ku, Chiba-shi, Chiba-ken 260-8717, Japan

Received 3 January 2003; accepted 3 January 2003

Abstract

Cancer cells are derived from their precursor cells, which normally develop to the matured cells to form individual organs. Neuroblastoma, one of the most common pediatric solid tumors, originates from possible cancer stem cells derived from the neural crest. During the development, neural crest cells segregate into several lineages such as sensory, enteric and sympathetic neurons. However, the genetic events to cause neuroblastoma occur only in the sympathetic precursor cells or cancer stem cells. Furthermore, spontaneous regression of a subset of neuroblastoma found in patients under one year of age mimics a developmentally programmed neuronal cell death that occurs in normal sympathetic neurons during the perinatal period. Thus, the genetic events to cause neuroblastoma may be programmed to occur in a lineage-specific as well as developmentally regulated manner. In this review, we discuss about the molecular link between neural development and the genesis of neuroblastoma based on our comprehensive genomics approach.

Keywords: Comprehensive genomics; Neuroblastoma cDNA project; Neural development

1. Introduction

Neuroblastoma (NBL) is one of the most common childhood cancers and is originated from the sympathetic precursor cells derived from the neural crest [1]. The clinical behavior of NBL is unique and enigmatic: the tumor cells spontaneously regress in patients under one year of age by undergoing differentiation and/or apoptosis, whereas the tumor often grows aggressively and eventually kills the patient when it occurs after one year of age [2,3]. It is thus mysterious why NBL regress or grow in an age-dependent manner. In 1963, Beckwith and Perrin have reported an interesting observation that only one of 40 microscopic fetal neuroblastomas has later become symptomatic, sporadic tumors. The remaining tumors disappeared spontaneously, suggesting that one of 250 (0.4%) fetuses has an 'in situ neuroblastoma' [4]. This observation may at least in part explain the result of NBL mass-screening performed in infants at the age of six months in Japan [5], because most of those tumors regress or take a favorable clinical course without decreasing the incidence of aggressive NBLs which are usually found in

* Corresponding author. Tel: +81-43-264-5431x5201; fax: +81-43-265-4459.
E-mail address: akiranak@chiba-ccri.chuo.chiba.jp (A. Nakagawara).

0304-3835/$ - see front matter © 2003 Elsevier Ireland Ltd. All rights reserved.
doi:10.1016/S0304-3835(03)00457-9

the patients over one year of age [6,7]. These have suggested that regression of NBL, which mimics the developmentally regulated 'programmed cell death (PCD)' of neurons [8,9], is still able to occur for about 12 months after birth. However, this idea cannot simply explain why NBLs found in the patients over one year of age do not regress.

It is highly possible that the molecular mechanism of normal development of sympathetic neurons is closely related to the regulation of NBL biology. Some important molecules of NBL, such as MYCN [10] and Trk [11], are already known to be the key players to regulate maturation of neural crest cells during development. However, we still miss a large number of genes or molecules playing important roles in the regulation of NBL biology and its genesis. In this review, we introduce a current knowledge about the molecular link between NBL and normal development of sympathetic cells, and discuss the future approaches to further understanding of the enigmatic tumor, NBL.

2. Neuronal lineage and oncogenic events

The oncogenic events to cause NBL appear to be strictly regulated and lineage-dependent, because NBL never occurs from the neural precursors of other than sympathoadrenal cell lineage (Fig. 1). The cell fate determination may be regulated by multiple transcription factors and their target genes which may include those of growth factors and their receptors [12,13]. The possible candidate genes to decide the direction of sympathetic differentiation include a human homolog of *Drosophila Acaete-Scute* proneural gene (hASH1) [14,15] and *Phox2a* [16,17] and *Phox2b* [18] of homeodomain genes. However, the precise mechanism is still elusive.

Another aspect of neuronal lineage specificity of the oncogenic events is shown by the mutation pattern of the *Trk* family genes [19]. *Trk* genes are specifically or preferentially expressed in neuronal tissues and cells. Nevertheless, the oncogenic *Trk* genes derived from translocation or somatic mutation have been exclusively observed in human malignancies with non-neuronal origin (colon cancer, papillary thyroid cancer, and acute myeloid leukemia). On the other hand, the expression levels of prototype Trk regulate the biology in cancers originated from neuronal precursor cells (neuroblastoma, medulloblastoma, thyloid C-cell hyperplasia and medullary thyroid cancer). Therefore, it should be interesting to know how the precursor cells choose the way to cause or regulate the cancer in a lineage-specific manner, that is absolutely unclear at this time.

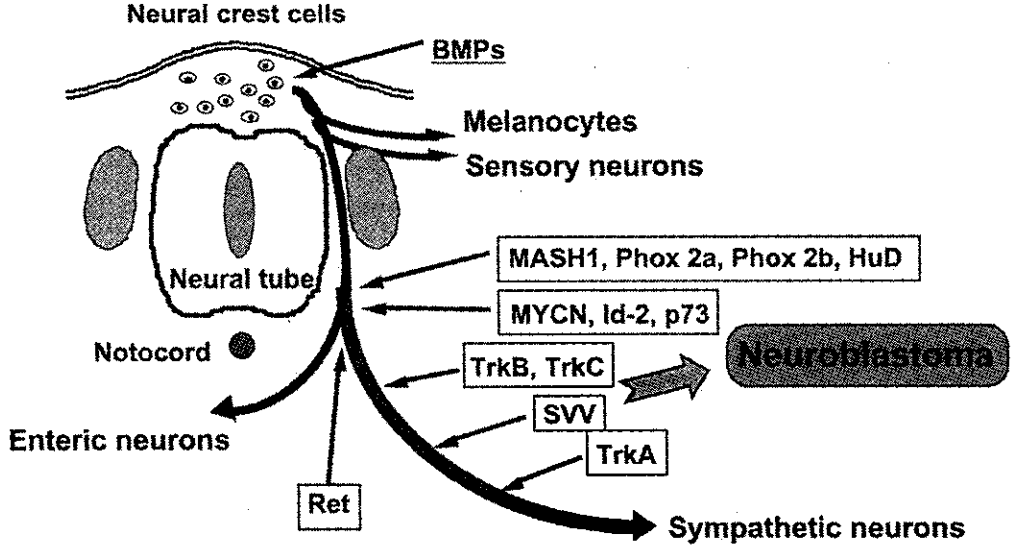

Fig. 1. Developmental lineages derived from the neural crest cells and the genesis of neuroblastoma.

3. Neural crest development and the molecules related to neuroblastoma

Neuroblastomas express many genes that are involved in the regulation of neural crest development [20–22]. The bone morphogenetic protein (BMP) signals regulate early stage of neural crest cell migration and differentiation before the decision to enter the sympathetic lineage [23], from which NBL exclusively arises. Of interest, the BMP signal is still functioning in many NBL cell lines because the treatment of the cells with BMP2 induced both phosphorylation of Smad1 and neurite outgrowth (Y. Nakamura, unpublished data). This suggests that NBLs still possess the ability to respond to the ligands that have worked at the early stage of normal neural development. Similarly, Delta/Notch signaling appears to function in NBLs by regulating neurite outgrowth [24]. Hypoxia, which induces dedifferentiation in NBL cells, decreased the expression of Notch1 [25].

hASH1 continues to be expressed at high levels in many neuroblastomas [26,27]. It is normally down-regulated after transient expression during the development of neural crest cells, that in turn promotes differentiation to the mature sympathetic neurons [28]. Targeted disruption of mouse homolog MASH1 has demonstrated the absence of sympathetic neurons [29], suggesting the important role of MASH1 expression in deciding the direction of sympathetic differentiation. Of interest, hASH1 is down-regulated during the NBL differentiation induced by retinoic acid [26,27]. hASH1 also directly represses expression of PACE4, a mammalian subtilin-like proprotein convertase that activates transforming growth factor (TGF)-β-related proteins such as BMPs [30]. This repression may shut off the BMP signaling and other factors in NBL cells. Expression of HES-1, a neuronal basic helix-loop-helix protein, represses hASH1 expression and leads the NBL cells to the status of de-differentiation [31]. As reported previously, MYCN targets Id-2 to induce its expression and the induced Id-2 inhibits the Rb tumor suppressor [32]. The still unidentified tumor suppressor(s) residing at the distal region of short arm of chromosome 1 might also be involved in this regulation because the allelic loss of the region is well correlated with amplification of *MYCN*[33,34]. The homeodomain transcription factors, Phox2a and Phox2b, are also essential for differentiation of noradrenergic neurons [35]. They may play a role in regulating the biology of NBL.

Other transcriptional regulators, that affect both neural crest development and NBL, include MYCN [36], hypoxia-inducible factor 1 (HIF-1) [37] and the tumor suppressors p53 [38] and p73 [39]. MYCN is frequently targeted to amplify in aggressive NBLs [40,41]. Since the importance of MYCN in NBL is invaluable, it is precisely discussed by M. Schwab in the separate chapter of this special issue.

4. NGF family signaling and the role of p53 and p73 in neuroblastoma

The downstream regulators of neural crest cell differentiation include neurotrophic factors and their receptors. Expression of neurotrophin receptors, TrkA and TrkB tyrosine kinases, strongly affects the biology of NBL [2,9]. TrkA, a high-affinity receptor for nerve growth factor (NGF), is expressed at high levels in NBLs of the patients with favorable prognosis, whereas it is extremely down-regulated in the tumors of those with unfavorable outcome [8,42–44]. In contrast, TrkB, a high-affinity receptor for brain-derived neurotrophic factor (BDNF), is preferentially expressed in aggressive NBLs especially with *MYCN* amplification [45]. The NBLs with high expression of TrkA frequently regress spontaneously by undergoing neuronal apoptosis as well as differentiation [8]. On the other hand, the NBLs with low expression of TrkA and amplification of *MYCN* often kill the patients. In such tumor cells, BDNF and TrkB promote tumor cell growth and metastasis in an autocrine manner [46]. Thus, the neurotrophic factors and their receptors, that normally regulate terminal differentiation of neural crest cells, may manipulate the differentiation and survival of the NBL cells [19].

Recent investigations have revealed that p53 and its family member p73 play a pivotal role in the developmentally regulated PCD of sympathetic neurons in mice [47]. The *p73*-deficient mice show neurological and immunological defects [48]. ΔNp73,

an N-terminally truncated form of p73 lacking transactivation ability, is predominantly expressed in developing brain and sympathetic neurons in mice and inhibits the neuronal PCD by blocking the proapoptotic function of p53 [47]. This observation has suggested p53, p73 and ΔNp73 to be the key regulators in the determination of neuronal differentiation and apoptosis. Interestingly, we and other investigators have recently found that p73 directly target *ΔNp73* for its expression by binding to the *ΔNp73* promoter. The induced *ΔNp73* then physically interacts with both p73 and wild type p53 to inhibit their function [49,50]. These relationships have suggested the presence of a negative feedback regulation of TAp73 by its target ΔNp73 in modulating cell survival and death of sympathetic neurons as well as NBL cells. c-Myc has also been involved in this regulatory system [51]. Since it is well recognized that the PCD of sympathetic neurons is strongly regulated by NGF signaling, elucidation of the downstream regulatory mechanism of the signaling by p53, p73 and ΔNp73 may become more important than ever. This may also help to understand the NBL biology regulated by NGF/TrkA signaling (Fig. 2). In NBL, the chromosome 1p36 region, to which p73 is mapped, is frequently deleted in advanced stage tumors. Furthermore, ΔNp73 is expressed at higher levels in unfavorable NBLs than in favorable ones [52]. In addition, according to the accumulating evidence, p73 may be one of the key factors of neural stem cells. Therefore, p73 could also be an important gene linking between neural development and cancer.

5. Comprehensive genomics of neuroblastoma

The rapid progress of the human genome project has enabled us to challenge the dynamic approaches to understanding of molecular genetic as well as cellular mechanism of cancers. It has also opened the door to unveil the molecular mechanism of neural development and neurogenic cancers. In NBL, the first trial to collect a large number of genes expressed in the CHP134 cell line was performed by K. Matsubara's group in Japan more than 10 years ago [20]. The cDNAs thus identified were published in 'Bodymap', the human gene expression database (http://bodymap.ims.u-tokyo.ac.jp/), including the information on gene expression in various tissues or cell types. Recently, R. Versteeg's group in Holland has introduced the method of serial analysis of gene

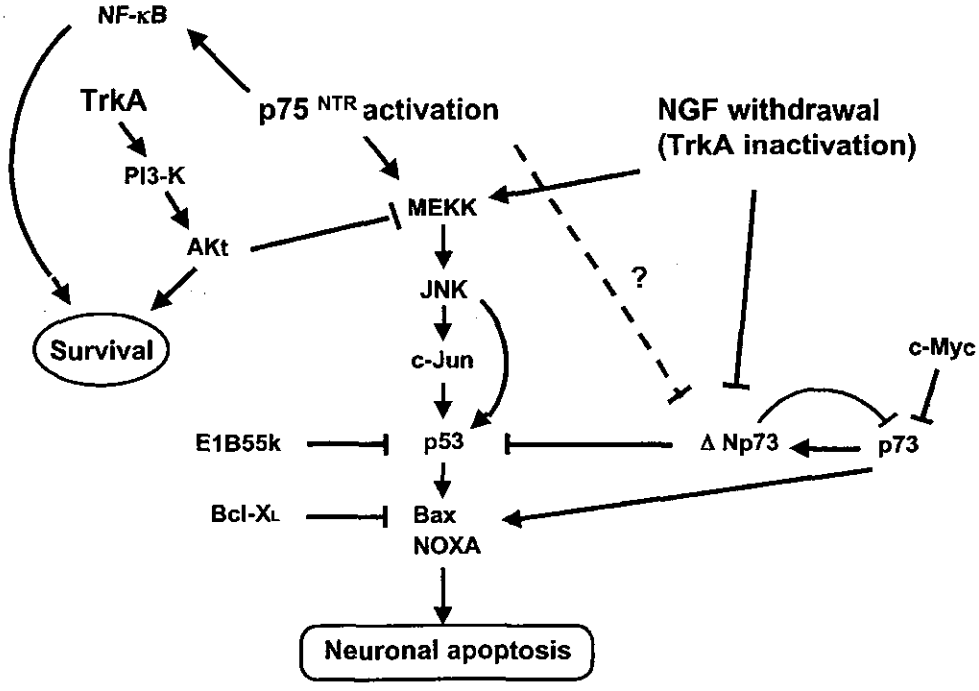

Fig. 2. The role of p53, p73 and ΔNp73 in intracellular signaling of neuronal survival and apoptosis mediated by NGF and its receptors.

Table 1
Summary of the neuroblastoma cDNA project

Number of the total clones	9,729
Number of the gene clusters	6,252
Differentially expressed genes between favorable and unfavorable subsets	
Function, known	255/1,325 (19%)
Function, unknown	502/2,115 (24%)
Total	757/3,440 (22%)
Nervous system-specific genes	156/2,297 (7%)

expression (SAGE) to identify the genes expressed in primary NBLs and cell lines in a large scale [53]. They have successfully found MEIS as an amplified gene in NBL and also identified the *MYCN* target genes [54]. Thus, the SAGE procedure is powerful for identifying the already known genes. However, it is not suitable for the approach to determine the novel genes whose functions are elusive. Therefore, we have decided to identify the individual genes expressed in the typical subsets of primary NBLs by starting the 'NBL cDNA project' which directly clones the expressed genes in a large scale from the NBL oligo-capping cDNA libraries [21,22]. In this review, we briefly present the results of and discuss about 6,252 gene clusters identified from the screening of 9,729 clones randomly picked up from three different NBL cDNA libraries: three favorable (F: stage 1, high expression of *TrkA* and a single copy of *MYCN*), three unfavorable (UF: stage 3 or 4, decreased levels of *TrkA* expression and amplification of *MYCN*) and a typical stage 4s (4s: high expression of *TrkA* and a single copy of *MYCN*) NBL libraries. This is the extended result of the previous report [22] that analyzed 4,243 cDNA clones randomly picked up from the F and UF NBL cDNA libraries.

5.1. A large scale cloning of the expressed genes from different subsets of primary neuroblastomas (Neuroblastoma cDNA project)

We randomly obtained 2,410, 2,244 and 5,075 cDNA clones from F, UF and 4s cDNA libraries and successfully sequenced the both or either end of 2,134, 2,109 and 5,004 clones, respectively (Table 1). We identified an extremely high number of 2,115 genes with unknown function compared with that (8%) found in the genes obtained from the cDNA libraries of childhood hepatoblastomas (HBLs) made by the same procedure (unpublished data). Interestingly, the average size of the genes obtained from NBLs (neuronal) was significantly larger than that from HBLs (hepatic) with an obvious tendency. We screened the genes for differential expression between F and UF NBLs by using semi-quantitative RT-PCR (16 F and 16 UF NBL samples) and found that 255 out of 1,325 known genes as well as 502 out of 2,115 novel genes were differential. In addition, RT-PCR analysis for expression in multiple human tissues showed that 156 of 2,297 genes, most of which were novel, displayed specific expression in neuronal tissues.

5.2. Expression profile and identification of the differentially expressed genes among the subsets

The expression profile of known genes was very different among the three subsets of NBL. The F subset frequently expressed neuronal specific genes including those related to neural differentiation, synapse, catecholamine metabolism, and protein degradation. On the other hand, the UF subset expressed many genes related to cell cycle control, protein synthesis and transcriptional regulation. The 4s tumor just before starting rapid regression also showed an extremely unique expression profile. It contained many apoptosis-related genes (*Bcl-10, NIP1, NIP3L, BAG-1, BID, FADD*, etc.), oncogenes (*c-Abl, c-Fos, K-Ras, c-Raf*, etc.), the other tumor-related genes (*TrkA, TGF-β, EXT2, LEU5, TNFR1, TRAP-1, ING-1, TRAIL*, etc.) and HLA family members that might be derived from the infiltrated lymphocytes into the tumor. Since the number of the genes cloned in our system was so small as compared to that of the SAGE method, we decided to examine whether or not the individual gene was expressed differentially between F and UF NBLs by using semi-quantitative RT-PCR.

The significance of the 757 differentially expressed genes was strongly implicated in understanding of NBL biology. Surprisingly, most of the genes were expressed at higher levels in F than UF subset [22]. The genes highly expressed in F subset contained those related to neuronal differentiation, migration, cell–cell interaction, protein degradation, synaptic

vesicles, catecholamine metabolism and intracellular signaling. Most of them define the neuronal-specific phenotype and maintain the neuronal function. They also included heat shock proteins and ubiquitin/proteasome-related molecules that might sense the stress. On the other hand, only about 10% of the differential genes were expressed at high levels in UF subset. The protein products of such known genes contained many transcriptional and translational regulators including oncoproteins. Notably, downregulation of dopamine-β-hydroxylase (DBH) and monoamine oxidase (MAO), the genes involved in the regulation of catecholamine metabolism, in UF as compared to F tumors could explain the previous observation that aggressive NBLs with *MYCN* amplification were dopaminergic [55].

5.3. Screening of the genes regulated by NGF in the newborn mouse SCG neurons

It is well accepted that both membrane receptors for NGF, TrkA and p75, are highly expressed in the F subset of NBL whereas they are strongly downregulated in the UF tumors with *MYCN* amplification [8,9]. The spontaneous regression only occurs in F type of NBLs, suggesting that the molecular mechanism of NBL regression is closely related to that of the PCD occurring in the late embryonic stage of sympathetic neurons. Indeed, the F type NBL expresses high levels of TrkA and p75 receptors but only a trace amount of NGF which might be supplied from the stromal cells such as Schwannian cells and fibroblasts within the tumor tissue [9]. The possible hypothesis is that only the tumor cells, which have obtained the limited amount of NGF, could survive and differentiate to ganglion-like mature cells, whereas the most cells, which have not been able to get enough amount of NGF to survive, might die. This attractive hypothesis prompted us to examine whether the differentially expressed genes between F and UF change their expression levels during the NGF-induced differentiation and the NGF-depletion-induced apoptosis in the newborn mouse superior cervical ganglion (SCG) neurons which are extremely sensitive to NGF for survival and death [56]. Among 353 genes we selected from the novel genes with differential expression, we could find 234 mouse counterparts, of which 181 primer pairs worked. They were subjected to screen for the change of expression by using semi-quantitative RT-PCR. Interestingly, seven and six genes were up- and down-regulated after NGF-induced differentiation, respectively, while one and 35 genes were up- and down-regulated after NGF depletion-induced apoptosis, respectively. Eight genes were up-regulated during NGF-induced differentiation and subsequently down-regulated after depletion of NGF, whereas 12 genes were down-regulated during the differentiation and then up-regulated after induction of apoptosis. However, 112 genes did not show any change in their expression in this system. The further analyses of those genes should give important insights into understanding of the differentiation and regression of NBL.

5.4. Chromosomal mapping of the differentially expressed genes

NBL is a cancer with extensive genomic aberrations [33,34]. According to the previous investigations, it is evident that the developmentally important genes like *MYCN* are targeted to cause NBL. Therefore, in order to identify more genes related to the NBL genesis, we mapped the 719 differentially expressed genes to human chromosomes (Fig. 3). It is obvious that there are some clusters of the differential genes in many loci on the chromosomes. The gene density mapped to each chromosome is also not the same. The genes receiving epigenetic regulations such as methylation and acetylation could also be included. The indicated mapping may give some hints for the future researches identifying important genes of NBL as well as those functioning in neural development.

5.5. cDNA microarray and array comparative genomic hybridization (array CGH)

We have recently developed our own cDNA microarray for investigation of NBL biology and mechanism of neuronal development. As many important genes of transcriptional regulator are involved, it may be useful to understand the complicated neural network during the normal